The American Journal of Pathology, Vol. 176, No. 4, April 2010

DOI: 10.2353/ajpath.2010.090829

Tumorigenesis and Neoplastic Progression

Endogenous Angiogenesis Inhibitor Vasohibin1 Exhibits Broad-Spectrum Antilymphangiogenic Activity and Suppresses Lymph Node Metastasis

Takahiro Heishi,* Tomoko Hosaka,* Yasuhiro Suzuki,* Hiroki Miyashita,* Yuichi Oike,† Takashi Takahashi,‡ Takumi Nakamura,§ Shingo Arioka,§ Yuichi Mitsuda,§ Tomoaki Takakura,§ Kanji Hojo,§ Mitsunobu Matsumoto,§ Chihiro Yamauchi,§ Hideki Ohta,§ Hikaru Sonoda,§ and Yasufumi Sato*

From the Department of Vascular Biology, Institute of Development, Aging, and Cancer, Tohoku University, Sendai, the Department of Molecular Genetics,† Graduate School of Medical Sciences, Kumamoto University, Kumamoto; the Division of Molecular Carcinogenesis,‡ Center for Neurological Diseases and Cancer, Nagoya University Graduate School of Medicine, Nagoya; and the Discovery Research Laboratories,§ Shionogi & Co. Ltd., Osaka, Japan*

During cancer progression, the angiogenesis that occurs is involved in tumor growth and hematogenous-distant metastasis, whereas lymphangiogenesis is involved in regional lymph node metastasis. Angiogenesis is counterregulated by various endogenous inhibitors; however, little is known about endogenous inhibitors of lymphangiogenesis. We recently isolated vasohibin1 as an angiogenesis inhibitor intrinsic to the endothelium and further demonstrated its anticancer activity through angiogenesis inhibition. Here, we examined the effect of vasohibin1 on lymphangiogenesis. Vasohibin1 exhibited broad-spectrum antilymphangiogenic activity in the mouse cornea induced by factors including VEGF-A, VEGF-C, FGF2, and PDGF-BB. We then inoculated highly lymph node–metastatic cancer cells into mice and examined the effect of vasohibin1 on lymph node metastasis. Tail-vein injection of adenovirus containing the human *vasohibin1* gene inhibited tumor lymphangiogenesis and regional lymph node metastasis. Moreover, local injection of recombinant vasohibin1 inhibited lymph node metastasis. These results suggest vasohibin1 to be the first known intrinsic factor having broad-spectrum antilymphangiogenic activity and indicate that it suppresses lymph node metastasis. *(Am J Pathol 2010, 176:1950–1958; DOI: 10.2353/ajpath.2010.090829)*

Peripheral lymphatic vessels, which are composed of a single layer of lymphatic endothelial cells (LECs) without mural cell coverage, collect fluid lost from blood vessels and maintain immune responses, lipid uptake, and tissue homeostasis.[1] Recently, attention has focused on lymphangiogenesis, which is the formation of new lymphatic vessels, because it has been shown to be related to lymph node (LN) metastasis of cancers.[2] Metastasis of malignant tumors to regional LNs is one of the early signs of spreading cancer, and it occurs as frequently as hematogenous distant metastasis.[3]

The formation of blood and lymphatic vessels is primarily controlled by vascular endothelial growth factor (VEGF) family members.[4] This family of growth factors consists of 5 members (ie, VEGF-A, VEGF-B, VEGF-C, VEGF-D, and placental growth factor). There are also 3 types of VEGF receptor (VEGFR) tyrosine kinases: VEGFR1, VEGFR2, and VEGFR3. The most important molecule in the VEGF family that mediates angiogenesis of the formation of new blood vessels is VEGF-A, and VEGFR2 is the major mediator of VEGF-A–driven responses in blood endothelial cells (BECs). Alternatively, the most important factors that mediate lymphangiogenesis are VEGF-C and VEGF-D, and VEGFR3 is the major mediator of VEGF-C– and VEGF-D–mediated responses in LECs.[4] In addition, several factors such as fibroblast growth factor (FGF)2, platele-derived growth factor BB (PDGF-BB), insulin-like growth factor 1

Supported by a grant from the program Grants-in-Aid for Scientific Research on Priority Areas from the Japanese Ministry of Education, Science, Sports, and Culture; by Health and Labor Sciences research grants; and by funding from Third Term Comprehensive Control Research for Cancer from the Ministry of Health, Labor, and Welfare (Japan).

Accepted for publication December 11, 2009

Address reprint requests to Yasufumi Sato, M.D., Ph., Department of Vascular Biology, Institute of Development, Aging, and Cancer, Tohoku University, 4-1, Seiryo-machi, Aoba-ku, Sendai 980-8575, Japan. E-mail: y-sato@idac.tohoku.ac.jp.

(IGF1), and hepatocyte growth factor (HGF) are reported to induce both angiogenesis and lymphangiogenesis.[5–8]

Angiogenesis is counterbalanced by various endogenous inhibitors.[9] However, little is known about endogenous inhibitors of lymphangiogenesis. Thrombospondin 1 (TSP1), an angiogenesis inhibitor, does not inhibit lymphangiogenesis.[10] Endostatin, another angiogenesis inhibitor, inhibits lymphangiogenesis and LN metastasis of certain tumors, but its effect on lymphangiogenesis is mediated via the down-regulation of VEGF-C in tumor cells.[11,12]

Recently, while searching for novel and functional VEGF-A–inducible molecules in endothelial cells (ECs), we identified an intrinsic inhibitor of angiogenesis in the vascular endothelium and named it vasohibin (VASH).[13] Thereafter we isolated a homologue of VASH, and so we designated it as VASH2 and renamed the original VASH as VASH1.[14] Our subsequent analysis revealed that VASH1 is expressed in BECs in the termination zone to halt angiogenesis, whereas VASH2 is expressed in infiltrating mononuclear cells in the sprouting front to promote angiogenesis.[15] When applied exogenously, VASH1 effectively inhibits various kinds of pathological angiogenesis[13,16–18] and inhibits tumor growth.[13,18] Here, we examined whether VASH1 has any effect on lymphangiogenesis, and if so, on LN metastasis of tumors. Our present study provides evidence that intrinsic factor VASH1 exhibited broad-spectrum antilymphangiogenic activity and inhibited LN metastasis.

Materials and Methods

All of the animal studies were reviewed and approved by the committee for animal study at our institute in accord with established standards of humane handling of research animals.

Mouse Corneal Micropocket Assay

Mouse corneal micropocket assays were performed as described previously.[13] Briefly, 4-week-old male BALB/c mice (Charles River Laboratories Japan, Inc., Yokohama, Japan) were deeply anesthetized, and 0.3 μg of poly-2-hydroxyethyl methacrylate (HEME) pellets (Sigma, St. Louis, Mo, USA) containing either vehicle or 160 ng of VEGF-A ($VEGF_{165}$, Sigma), 160 ng of VEGF-$C_{Cys156ser}$ (R&D Systems, Inc., Minneapolis, MN), 12.5 ng or 80 ng of FGF2 (BD Biosciences, San Jose, CA), or 80 ng of PDGF-BB (R&D Systems, Inc.) was implanted in the corneas. A total of 4 ng of VASH1 protein was added or not to the pellets.

Fourteen days after the pellet inoculation, the corneas were excised, washed in PBS, and fixed in acetone at 4°C for 30 minutes. After three additional washings in PBS and blocking with 1% BSA in PBS for 1 hour, the corneas were stained overnight at 4°C with rabbit anti-mouse lymphatic vessel endothelial receptor 1 (LYVE1) antibody (1:500; Acris Antibodies GmbH, Hiddenhausen, Germany) and rat anti-mouse CD31 antibody (1:500; Research Diagnostics Inc., Flanders, NJ). On day 2, the corneas were washed, and secondary antibody reactions were performed by treatment with Alexa Fluor 488-conjugated donkey anti-rat IgG (1:1000; Invitrogen Corp., Carlsbad, CA) and Alexa Fluor 568-conjugated goat anti-rabbit IgG (1:1000; Invitrogen Corp.) for 6 hours at 4°C. After a last washing, the sections were covered with fluorescence mounting medium (DakoCytomation Inc., Carpinteria, CA). Double-stained whole-mount sections were observed under a FluoView FV1000 confocal microscope (Olympus Corp., Tokyo, Japan). Blood vessels were positive for CD31 antigen, and lymphatic vessels were positive for LYVE1. The area covered by blood and lymphatic vessels was measured by using NIH ImageJ software (v. 1.39u).

Subcutaneous Tumor Xenograft Model

Cells of the human lung cancer cell line NCI-H460-LNM35 (LNM35, 1.0×10^7 cells) were implanted into the subcutaneous tissue of the right abdominal wall of female SCID mice (6 to 8 weeks old, Charles River Laboratories, Japan). A replication-defective adenovirus vector encoding human *vasohibin1* (AdVASH1) or *β-galactosidase* gene (AdLacZ, 1×10^9 plaque-forming units [pfu]) was intravenously injected into a tail vein at day 0 and day 14 after the implantation.[17] Four weeks after the inoculation the mice were sacrificed, and tumors, along with some internal organs such as the trachea and axillary LNs, were collected. The sizes of axillary LNs were measured, and sections of the nodes were stained with hematoxylin and eosin to evaluate tumor metastasis.

Tissues were embedded in optimal cutting temperature (OCT) compound (Sakura Finetechnical, Tokyo, Japan) to make frozen tissue specimens, and sectioned at 6 μm. Samples were fixed with methanol for 20 minutes at −20°C, blocked with 1% BSA in PBS for 30 minutes at room temperature, and stained with anti-mouse LYVE-1 antibody (1:500), anti-mouse CD31 antibody (1:500), or anti-mouse F4/80 antibody (1:500; Acris Antibodies GmbH) at 4°C overnight. This action was followed by staining with secondary antibodies Alexa fluor 488 donkey anti-rat IgG (1:1000), Alexa fluor 568 goat anti-rabbit IgG (1:1000) and TO-PRO-3 iodide (1:1000; Invitrogen Corp.) for 30 minutes at room temperature. After having been washed three times with PBS, the sections were covered with fluorescence mounting medium and observed under an Olympus FluoView FV1000 confocal microscope. The vascular lumen was traced, and the vascular luminal area was analyzed with NIH ImageJ software.

Western Blotting of Human VASH1 Protein

Frozen tissues (vena cava, kidney, liver, lung, and heart) were homogenized and lysed with modified RIPA buffer. Mouse blood was heparinized and centrifuged to obtain plasma. Albumin and IgG were depleted from the plasma with a removal kit according to the manufacturer's protocol (Amersham Biosciences Corp., Piscataway, NJ). Thereafter, Western blot analysis was performed as described previously.[13] Horseradish peroxidase (HRP)-labeled anti-human VASH1 monoclonal antibody (clone 4E12) was used, which recognized human but not murine VASH1 protein.

ELISA for VASH1

Peptides corresponding to Gly286-Arg299 (VC1) and Ala217-Lys229 (VR) of human VASH1 protein were conjugated with keyhole limpet hemocyanin. These antigens were used to immunize A/J mice, and several monoclonal antibodies were prepared as described previously.[13] We examined various combinations of monoclonal antibodies and found that the combination of VC1-derived clone 12F6 and VR-derived clone 12E7 was ideal for a highly sensitive and specific ELISA system that could detect human and mouse VASH1 protein equally. We used 12F6 and 12E7 for plate coating and HRP labeling, respectively. The detailed procedure for the measurement was described previously.[19]

Preparation of Recombinant VASH1 Protein

Human *VASH1* gene with optimized codons for *Escherichia coli (E. coli)* expression was cloned in pET-32 LIC/Xa (Novagen, Madison, WI). The resultant expression plasmid encoded *VASH1* with a sequence of GSNSPLAMAISDPNSSSVDKLAAALEHHHHHH at its C terminus. *E. coli* transformants were cultivated at 37°C in TB (2.4 M yeast extract, 1.2 Mtryptone, 1.25 M K_2HPO_4, 0.23 M KH_2PO_4, 500 μg/m/ polypropylene glycol #2000, 50 μg/ml ampicillin; pH 7.0) supplied with 4% glycerol, and the expression was induced by the addition of 1 mmol/L isopropyl β-D-1-thiogalactopyranoside (OD_{650} = 5). After a 16-hour cultivation, cells were collected and disrupted in 20 mmol/L sodium phosphate buffer, pH 7.6, containing 0.5 mol/L NaCl and 1 mmol/L phenylmethylsulfonyl fluoride in a high-pressure homogenizer. The inclusion bodies were collected, washed with the same buffer, and solubilized in 20 mmol/L sodium phosphate buffer, pH 8.0, containing 0.5 mol/L NaCl, 1 mmol/L phenylmethylsulfonyl fluoride, 5 mmol/L 2-mercaptoethanol, 60 mmol/L imidazole, and 7 mol/L guanidine-HCl. The soluble fraction was loaded onto a Ni Chelating Sepharose column (16 mm × 125 mm, GE health care, Carnegie Center, NJ) equilibrated with the above solubilization buffer except that the guanidine-HCl was replaced by 8 mol/L urea and eluted with the same buffer containing 300 mmol/L imidazole. VASH1 fusion protein fraction was dialyzed against 20 mmol/L glycine-HCl buffer, pH 3.5, and digested with coagulation factor Xa (Novagen) for 1 hour at

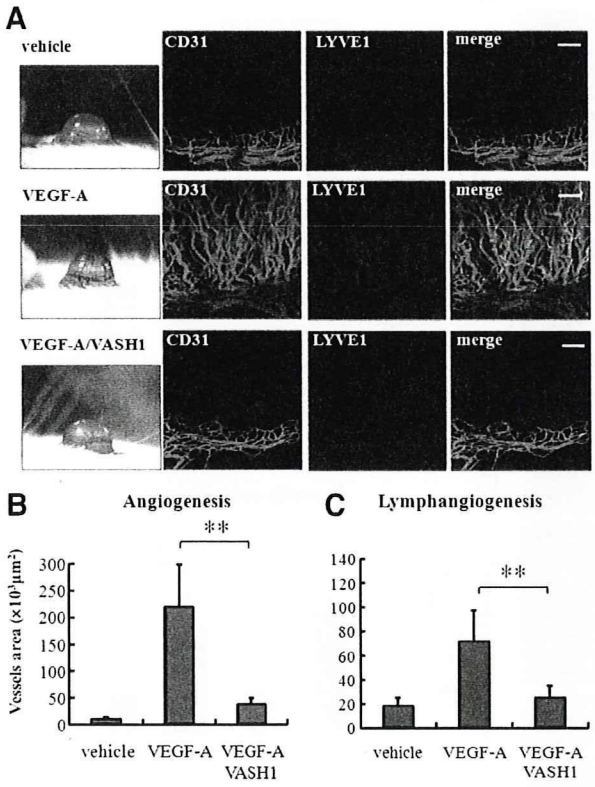

Figure 1. VASH1 inhibits angiogenesis and lymphangiogenesis induced by VEGF-A. **A:** Pellets containing 160 ng of VEGF-A plus or minus 4 ng of VASH1 were inoculated into the mouse cornea. Fourteen days after the inoculation, the corneas were harvested and immunostained for LYVE1 (red) or CD31 (green). Scale bar = 200 μm. Experiments were repeated at least 3 times, and representative data are shown here. **B:** The area of CD31-positive vessel was quantified; the means and SDs are shown. VASH1 significantly inhibited angiogenesis and lymphangiogenesis induced by VEGF-A. n = 5, $^{**}P < 0.01$. **C:** The area occupied by LYVE1-positive vessel was quantified, and the means and SDs shown. VASH1 significantly inhibited the lymphangiogenesis induced by VEGF-A. n = 5, $^{**}P < 0.01$.

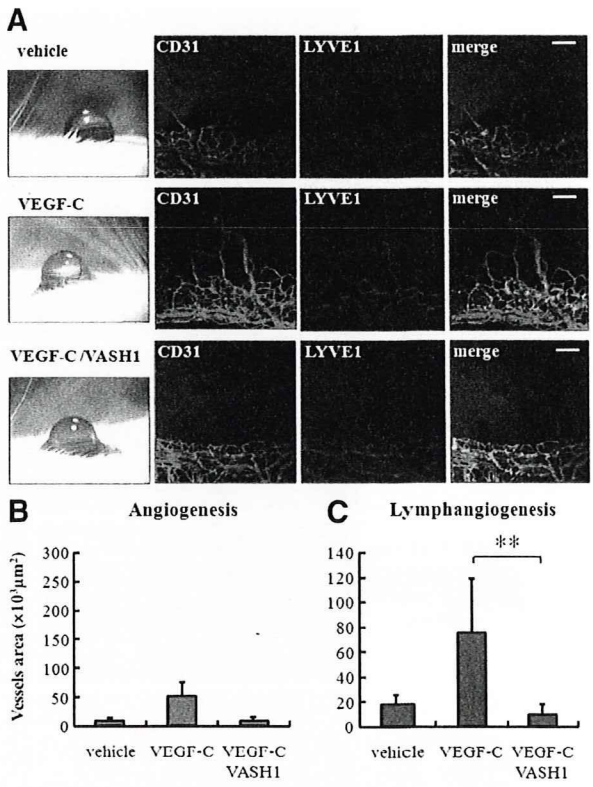

Figure 2. VASH1 inhibits angiogenesis and lymphangiogenesis induced by VEGF-C. **A:** Pellets containing 160 ng of VEGF-C plus or minus 4 ng of VASH1 were inoculated into the mouse cornea. Fourteen days after the inoculation, corneas were harvested and immunostained for LYVE1 or CD31. Scale bar = 200 μm. Experiments were repeated at least 3 times, and representative data are shown here. **B:** The area of CD31-positive vessel was quantified, and the means and SDs are shown. VEGF-C limitedly stimulated angiogenesis, as did VASH1, though no significant differences were observed. n = 5. **C:** The area of LYVE1-positive vessels was quantified, and the means and SDs are shown. VASH1 significantly inhibited the lymphangiogenesis induced by VEGF-C. n = 5, $^{**}P < 0.01$.

25°C. The released VASH1 protein was collected, solubilized, and purified with Ni Chelating Sepharose. VASH1 protein was then collected as the insoluble fraction after dialysis against 20 mmol/L Tris-HCl (pH 8.0), resolubilized in 25 mmol/L sodium phosphate (pH 7.2) containing 4 mol/L urea, loaded onto a Q Sepharose column (16 mm × 140 mm, GE health care), and eluted by linearly increasing the NaCl concentration to 1 mol/L. Finally, the VASH1 protein was dialyzed against 20 mmol/L glycine-HCl buffer (pH 3.5).

Orthotopic Tumor Xenograft Model

Human breast cancer cell line MDA-MB-231 obtained from American Type Culture Collection was transfected with firefly luciferase and geneticin resistance genes, and stable transfectants (231Luc-1 cells) were selected. 231Luc-1 cells were inoculated into the mammary fat pad of mice, and spontaneous LN metastatic cells (231LN-Luc-1 cells) were isolated from the axillary LNs and cultured.

231LN-Luc-1 cells (5×10^6) in 50 μl of 40% Hanks' balanced salt solution containing 50% Matrigel (Becton, Dickinson and Company, Franklin Lakes, NJ) and 10% VASH1 or human serum albumin (HSA) solution (5 μg protein/50 μl solution) were inoculated into the abdominal mammary fat pad of female C57BL-17/Icr SCID Jcl mice (CLEA Japan, Inc., Tokyo, Japan). Six days after the inoculation, 2.5 μg of VASH1 or HSA was locally injected into the abdominal mammary fat pad every 3 to 4 days. LN metastasis (axillary region) was analyzed on day 32 by a bioluminescence imaging technique. Fifty to 60 seconds after the luciferin injection, mice were placed in the IVIS Imaging System (Xenogen, Alameda, CA) and imaged. LN metastasis was quantified as photons/sec obtained with Living Image® software (Xenogen).

Calculations and Statistical Analysis

Data were expressed as the mean plus or minus SD. The significance of the data were determined by using Student *t* test for the evaluation of angiogenesis, lymphangiogenesis, plasma VASH1 concentration, and tumor-related photons, and by performing Fisher exact test

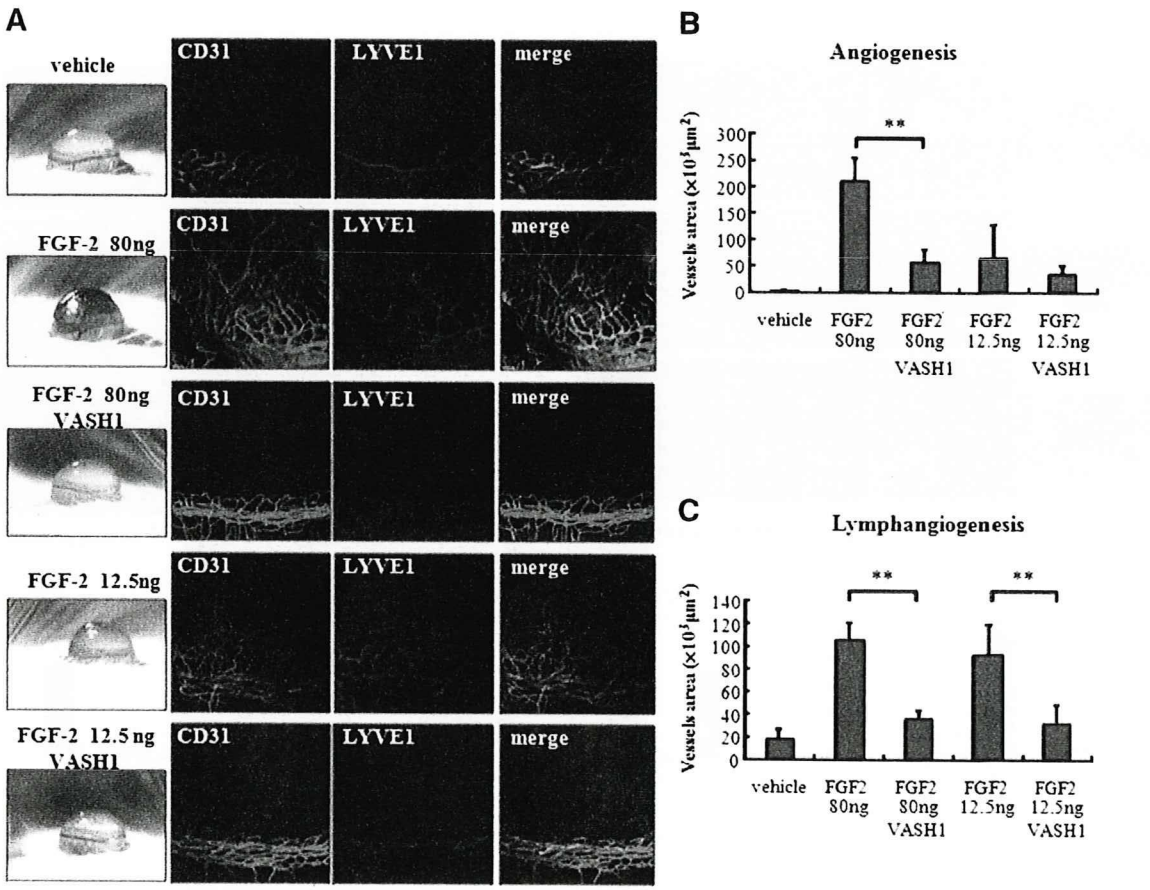

Figure 3. VASH1 inhibits angiogenesis and lymphangiogenesis induced by FGF2. **A:** Pellets containing 80 ng (high dose) or 12.5 ng (low dose) of FGF2 plus or minus 4 ng of VASH1 were inoculated into the mouse cornea. Fourteen days after the inoculation, the corneas were harvested and immunostained for LYVE1 (red) or CD31 (green). Scale bar = 200 μm. Experiments were repeated at least 3 times, and representative data are shown here. **B:** The areas of CD31-positive vessel were quantified, and the means and SDs are shown. At the higher dose, FGF2 induced angiogenesis, and VASH1 significantly inhibited the angiogenesis induced by FGF2. $n = 5$, $^{**}P < 0.01$. At the lower dose, FGF2 did not significantly induce angiogenesis. $n = 5$. **C:** The areas of LYVE1-positive vessel were quantified, and the means and SDs are shown. At both the higher and lower doses, FGF2 induced lymphangiogenesis, and VASH1 significantly inhibited the lymphangiogenesis induced by either dose of FGF2. $n = 5$, $^{**}P < 0.01$.

for the evaluation of lymph node metastasis. Statistical significance was defined as a P value less than 0.05.

Results

VASH1 Exhibits Broad-Spectrum Antiangiogenic and Antilymphangiogenic Activities

Earlier we used human VASH1 protein in various mouse models and showed its antiangiogenic activity.[13,16–18] A recent study indicated that the antiangiogenic effect of mouse VASH1 protein was not distinguishable from that of human VASH1 protein in a mouse model.[20] Here we used human VASH1 protein. VEGF-A strongly induces both angiogenesis and lymphangiogenesis in the mouse cornea.[21] By immunostaining a mouse cornea for CD31 as a marker for BECs and for LYVE1 as a marker for LECs, we confirmed this activity of VEGF-A (Figure 1A), and further showed that the co-administration of recombinant VASH1 protein with VEGF-A almost completely blocked VEGF-A–induced angiogenesis and lymphangiogenesis (Figure 1, B and C).

We next applied VEGF-C, a principal stimulator of lymphangiogenesis, to the mouse cornea. In agreement with a previous report,[5] VEGF-C induced lymphangiogenesis and also angiogenesis to some extent when administered alone to mouse corneas, and co-administration of VASH1 with VEGF-C abolished both lymphangiogenesis and angiogenesis induced by VEGF-C (Figure 2A). Quantitative analysis confirmed these effects of VASH1 (Figure 2, B and C).

We further administered growth factors other than VEGF family members that are known to have stimulatory effects on angiogenesis and lymphangiogenesis. It is reported that FGF2 induces both angiogenesis and lymphangiogenesis at a higher dose (80 ng per pellet), but primarily induces lymphangiogenesis at a lower dose (12.5 ng per pellet).[22] We confirmed these differential effects of FGF-2 and further demonstrated that co-administration of VASH1 with high-dose FGF2 almost completely blocked both angiogenesis and lymphangiogenesis (Figure 3, A–C). PDGF-BB is reported to induce intratumoral lymphangiogenesis and to promote lymphatic metastasis.[6] VASH1 inhibited both angiogenesis and lymphangiogenesis induced by PDGF-BB (Figure 4, A and B).

Taken together, these results indicate that VASH1 has broad-spectrum antiangiogenic and antilymphangiogenic activities.

VASH1 Inhibits Tumor Lymphangiogenesis and LN Metastasis

Next, we proceeded to test the effect of VASH1 in the tumor xenograft model. We injected adenovirus vector encoding the human *VASH1* gene (AdVASH1) into a tail vein of mice. Adenovirus vector encoding the *β-galactosidase* gene (AdLacZ) was used as a negative control. This vector should supply sufficient VASH1 protein to regulate angiogenesis, as described previously.[17] Indeed, Western blotting for human VASH1 revealed that human VASH1 protein accumulated in various organs 10 days after the viral injection (Figure 5A). Differences in molecular size should be attributable to the FLAG tag in recombinant VASH1 protein for control,[11] and posttranslational processing of VASH1 protein in mice.[19] ELISA analysis recognizing both murine and human VASH1 revealed that the plasma concentration of VASH1 increased about threefold (Figure 5B).

We then inoculated the flanks of SCID mice with highly LN-metastatic human non-small cell lung cancer (LNM35) cells.[23] Adenovirus vectors were injected on day 0 and day 14, and tumor tissues were collected on day 28. Tumor angiogenesis was analyzed by immunostaining VECs for CD31. Blood vessels were distributed within the tumor; and, as expected, the blood vessel area was significantly reduced in the AdVASH1-injected group (Figure 5C). Tumor lymphangiogenesis was analyzed by immunostaining for LYVE1. We simultaneously performed F4/80 immunostaining to distinguish LYVE1-expressing macrophages as described.[24] LYVE1-positive and F4/

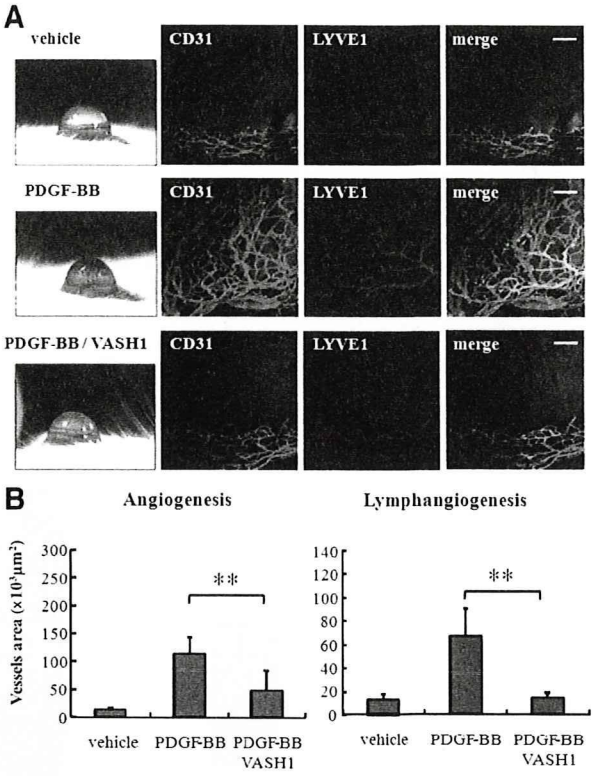

Figure 4. VASH1 inhibits angiogenesis and lymphangiogenesis induced by PDGF-BB. **A:** Pellets containing 160 ng of PDGF-BB plus or minus 4 ng of VASH1 were inoculated into the mouse cornea. Fourteen days after the inoculation, corneas were harvested and immunostained for LYVE1 or CD31. Scale bar = 200 μm. Experiments were repeated at least three times, and representative data are shown here. **B:** The area of CD31-positive vessel was quantified, and the means and SDs are shown. VASH1 significantly inhibited the angiogenesis induced by PDGF-BB. $n = 5$, $^{**}P < 0.01$. The area of LYVE1-positive vessel was quantified, with means and SDs shown. VASH1 significantly inhibited the lymphangiogenesis induced by PDGF-BB. $n = 5$, $^{**}P < 0.01$.

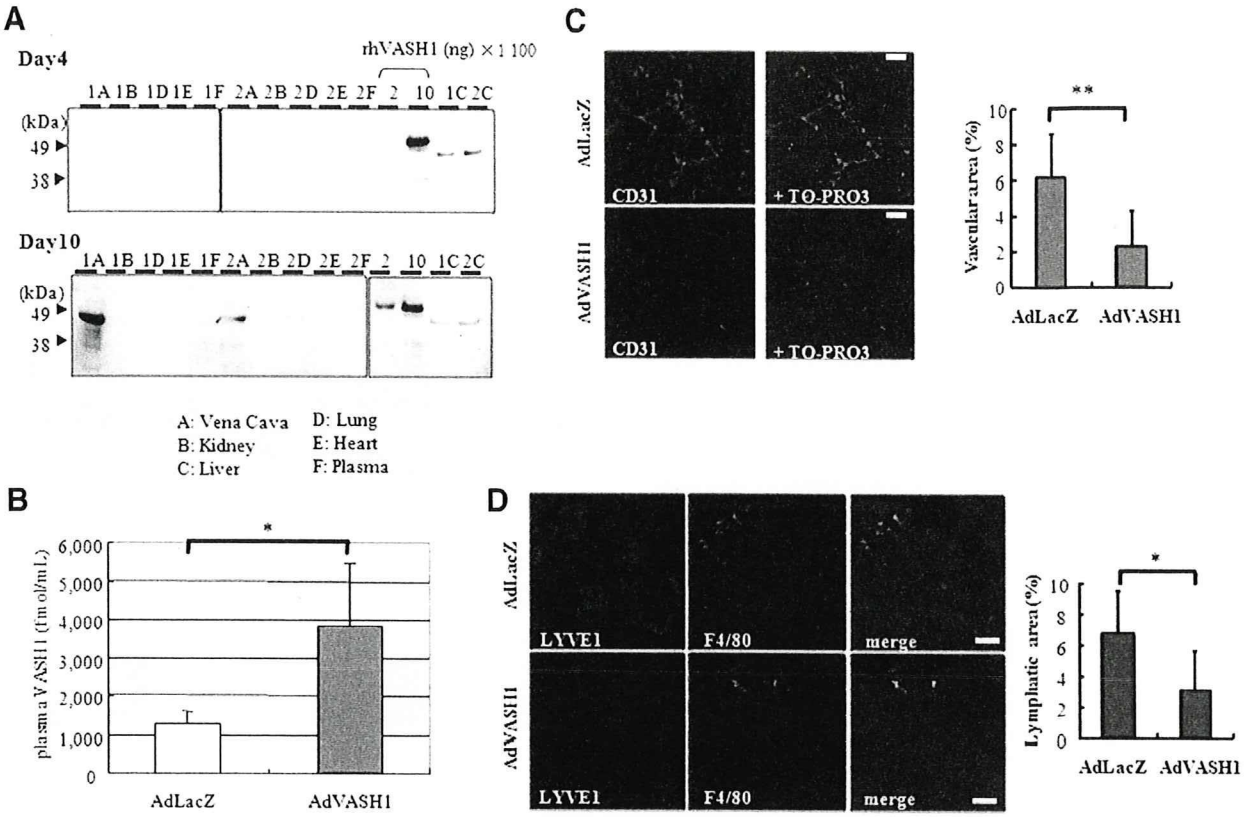

Figure 5. Adenovirus-mediated systemic delivery of VASH1 protein inhibits tumor lymphangiogenesis of LNM35 cells. **A:** AdVASH1 or AdLacZ (1×10^{9} pfu) was injected into a tail vein of mice. Various organs were collected from two mice on day 4 and day 10 after the injection, and Western blotting for human VASH1 protein was performed as described in *Materials and Methods*. Recombinant human VASH1 protein with a triple repeat of the FLAG tag (rhVASH1) was used as a control. **B:** Plasma samples were collected 10 days after the injection, and the concentration of VASH1 was determined by ELISA. $n = 5$, $^{*}P < 0.05$. **C:** LNM35 cells were inoculated subcutaneously, and adenovirus vectors were injected into the tail vein of mice on day 0 and day 14. On day 28, the mice were sacrificed and tumors were resected. Tumor sections were immunostained for CD31 (green), and TO-PRO3 (blue) was used for nuclear staining. Scale bar = 200 μm. The intratumoral CD31-positive vascular area was quantified and expressed as % of a field. The means and SDs are shown. Tumor angiogenesis was significantly inhibited in the AdVASH1-injected mice. $n = 13$ (AdLacZ), $n = 12$ (AdVASH1), $^{**}P < 0.01$. **D:** Tumor sections were immunostained for LYVE1 (red) and F4/80 (green). TO-PRO3 (blue) was used for nuclear staining. Scale bar = 100 μm. The peritumoral LYVE1-positive and F4/80-negative vascular area was quantified and expressed as % of a field. The means and SDs are shown. Tumor lymphangiogenesis was significantly inhibited in the AdVASH1-injected mice. $n = 13$ (AdLacZ), $n = 12$ (AdVASH1), $^{*}P < 0.05$.

80-negative lymphatic vessels were distributed in the peri-tumoral region (Figure 5D). Quantitative analysis revealed that lymphatic vessels in the peritumoral region were significantly reduced in area in the AdVASH1-injected group (Figure 5D).

The regional axillary LNs were recovered on day 28. LN size was measured, and LN metastasis was determined by histological analysis. VASH1 significantly inhibited LN metastasis, as LN metastasis occurred in 14 of 17 AdLacZ-injected mice, but in only 4 of 16 AdVASH1-injected mice (Figure 6A). It has been described that lymphangiogenesis in the regional LNs occurs before LN metastasis and determines tumor dissemination beyond the regional LNs.[25,26] Recovered LNs were therefore immunostained for CD31 and LYVE1 to analyze angiogenesis and lymphangiogenesis (Figure 6B). Angiogenesis was not increased in either metastasis-negative or metastasis-positive LNs when compared with LNs isolated from non–tumor-bearing mice (normal LNs), but was significantly decreased in AdVASH1-injected mice when compared with the AdLacZ-injected mice (Figure 6C). In contrast, lymphangiogenesis was significantly augmented in the metastasis-negative LNs of the AdLacZ-injected mice, and was abolished in those the AdVASH1-injected mice (Figure 6C). These results suggest that VASH1 inhibited lymphangiogenesis in regional LNs before the establishment of LN metastasis.

We tested whether VASH1 impaired normal vessels in mice. Tracheal mucosa was immunostained for CD31 and LYVE1. We did not detect any morphological changes in blood or lymphatic vessels of mice injected with AdVASH1 (Figure 7A) Quantitative analysis revealed that VASH1 did not alter the area of blood or lymphatic vessels (Figure 7B).

To further show the effect of VASH1 on LN metastasis, we performed orthotopical inoculation of LN metastatic human breast cancer (231LN-Luc-1) cells. Moreover, because of the limitation of the gene therapy approach in cancers, we applied recombinant VASH1 protein. We inoculated 231LN-Luc-1 cells into the abdominal mammary fat pad of mice in the presence of recombinant VASH1 protein. We then injected recombinant VASH1 protein locally, because of the obstacle of using recombinant VASH1 protein for systemic administration. There

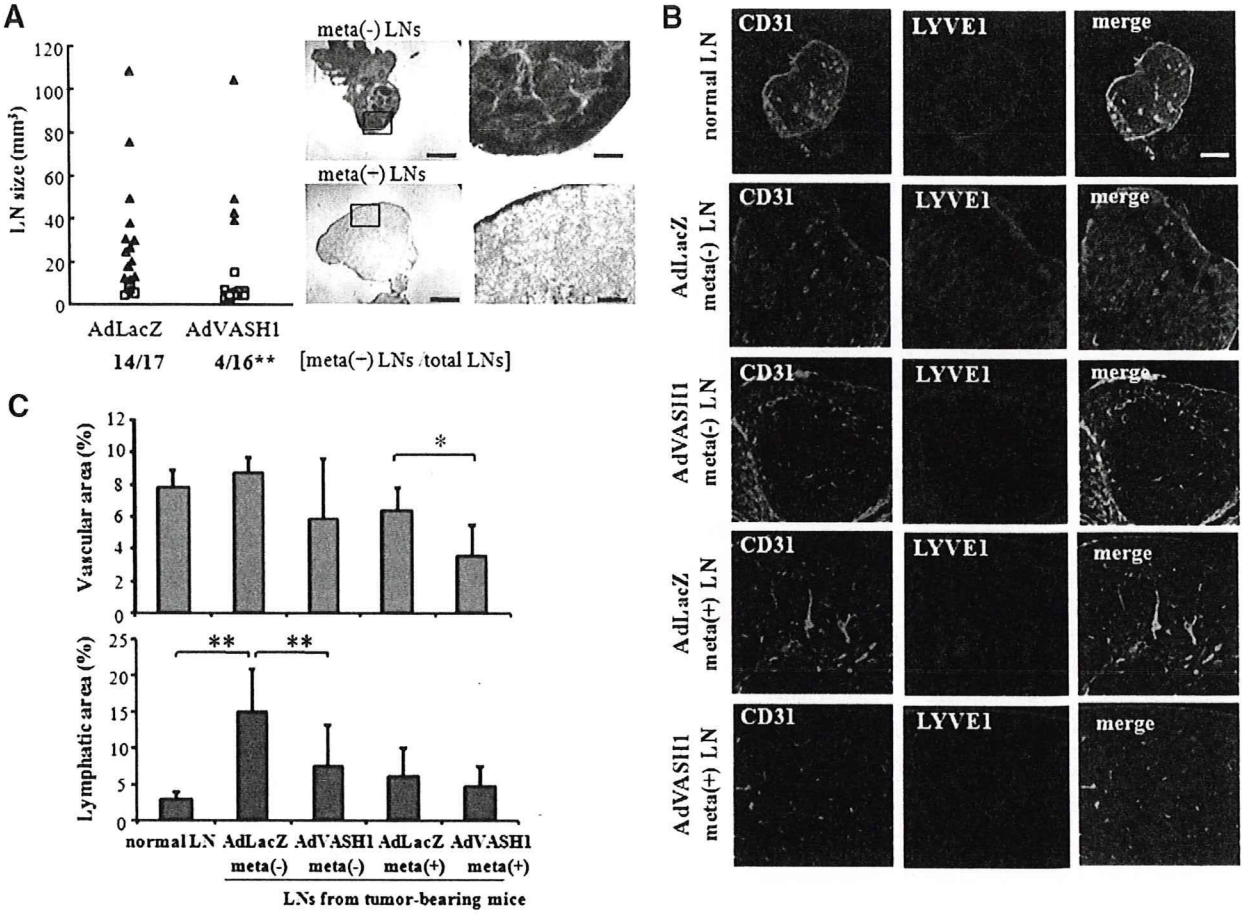

Figure 6. VASH1 inhibits LN metastasis of subcutaneously inoculated LNM35 cells. **A:** Axillary LNs were recovered. LN size was measured, and the size of LNs and the presence or absence of LN metastasis is shown. The frequency of LN metastasis in AdVASH1-injected mice was significantly lower, $^{**}P < 0.01$. Experiments were repeated three times, and representative data are shown here. LN metastasis was determined by histological analysis. Boxed fields on the left were enlarged and shown on the right. Scale bars = 500 μm on the left and 100 μm on the right. **B:** LNs were immunostained for CD31 (green) and LYVE1 (red). TO-PRO3 (blue) was used for nuclear staining. Scale bar = 200 μm. **C:** The CD31-positive and LYVE1-positive vessel areas were quantified and expressed as % of a field. The means and SDs are shown. The area of lymphatic vessels was significantly decreased in the metastasis-negative LNs of the AdVASH1-injected mice, whereas the area of blood vessels was significantly decreased in the metastasis-positive LNs of the AdVASH1-injected mice. $n = 8$ (AdLacZ meta+ and AdVASH1 meta-), $n = 4$ (normal LN, AdLacZ meta- and AdVASH1 meta+). $^{*}P < 0.05$, $^{**}P < 0.01$.

was a significant decreased in the bioluminescence in the VASH1-injected group (Figure 8).

Discussion

VASH1 was originally isolated as a VEGF-A–inducible angiogenesis inhibitor.[13] Here we assessed the effect of VASH1 on lymphangiogenesis, and explored its broad-spectrum antiangiogenic and antilymphangiogenic activities. Our findings are the first demonstration that a molecule intrinsic to the endothelium exhibits such activities.

We first applied VASH1 in combination with VEGF-A to the mouse cornea. VEGF-A induced both angiogenesis and lymphangiogenesis, and co-administration of VASH1 abolished those effects of VEGF-A. VEGF-A can induce lymphangiogenesis by affecting LECs directly or indirectly.[27,28] One means by which VEGF-A indirectly induces lymphangiogenesis is by mediating angiogenesis, which increases the local accumulation of inflammatory cells and thus the supply of lymphangiogenic factors such as VEGF-C.[29–31] Because VASH1 inhibited angiogenesis, VASH1 might exhibit its antilymphangiogenesis activity via the indirect route. To further clarify the effect of VASH1 on lymphangiogenesis, we replaced VEGF-A with VEGF-C, a principal and direct lymphangiogenesis stimulator. The result showing that VASH1 inhibited VEGF-C–stimulated lymphangiogenesis supports the direct antilymphangiogenesis activity of VASH1. Notably, VASH1 inhibited FGF2- and PDGF-BB–induced angiogenesis and lymphangiogenesis as well. Thus, the inhibitory effect of VASH1 is not restricted to the phenomena induced by the VEGF family members.

We focused our attention on the antilymphangiogenic activity of VASH1, as tumor lymphangiogenesis is recognized as a therapeutic target for the prevention of LN metastasis. We experimentally used an adenovirus vector, and showed that VASH1 delivered by this means inhibited tumor lymphangiogenesis and LN metastasis in a mouse xenograft model. The injection of

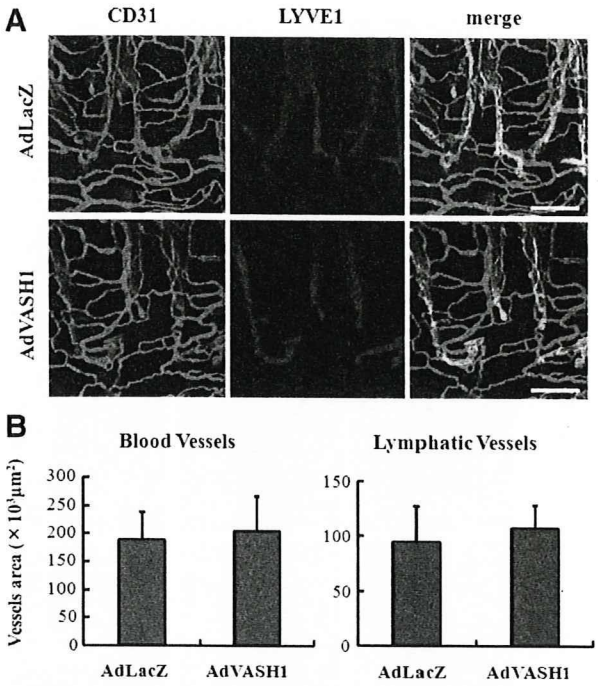

Figure 7. VASH1 does not damage normal vessels. **A:** A mouse trachea was collected on day 28, and its mucosa was immunostained for CD31 (green) and LYVE1 (red). Scale bar = 200 μm. No morphological changes were evident in the AdVASH1-injected mice. **B:** The areas of blood vessels and lymphatic vessels were quantified, and the means and SDs are shown. $n = 5$. No changes in blood or lymphatic vascular areas were evident.

AdVASH1 via a tail vein caused the synthesis of VASH1 protein in the liver. The accumulation of human VASH1 protein detected in various organs indicates that this procedure allowed us to supply human VASH1 protein systemically. The high affinity of VASH1 for heparin should be the reason for this local accumulation.[19]

As expected, AdVASH1 inhibited tumor lymphangiogenesis and regional LN metastasis. We further tested lymphatic vessels in the regional LNs, and found that lymphangiogenesis was significantly augmented in the metastasis-negative LNs and was inhibited by AdVASH1. However, lymphangiogenesis was no more augmented in the metastasis-positive LNs in the AdLacZ control. We speculate that this decrease in lymphatic vessels in the metastasis-positive LNs in the AdLacZ control might be attributable to the occupation of LNs by metastatic cancer tissues (Figure 6A), as lymphatic vessels are rarely present within cancer tissues.[32]

We previously reported the antitumor effect of VASH1 to occur through inhibition of angiogenesis.[13,18] Antiangiogenic therapy is currently being used clinically to inhibit tumor angiogenesis and tumor growth by targeting VEGF-A–mediated signaling, but one of the problems with this treatment is drug resistance.[33,34] Cancer cells switch to producing other factors such as FGF2 to combat the antiangiogenic therapy when they are treated with VEGF-A targeting monotherapy.[33] PDGF-mediated signaling is another pathway that is activated in cancers.[35] Importantly, FGF2 and PDGF-BB synergistically promote tumor neovascularization and distant metastasis.[36] The fact that VASH1 exhibited broad-spectrum antiangiogenic activity, including that against FGF2 and PDGF-BB, reveals an advantageous characteristic of it.

It has been reported that the blockade of VEGFR3 signaling inhibits tumor lymphangiogenesis and LN metastasis.[37] Thus, with analogy to the antiangiogenesis therapy, VEGFR3 signaling is proposed to be an appropriate target for the inhibition of lymphangiogenesis. It is not clear yet whether resistance would occur when VEGFR3 signaling is blocked.[37] Nevertheless, because FGF2 and PDGF-BB, which are candidates to cause drug resistance in antiangiogenic therapy, promote lymphangiogenesis as well, the broad-spectrum antiangiogenic and antilymphangiogenic activities of VASH1 are noteworthy.

In summary, our present study shows that the intrinsic factor VASH1 has broad-spectrum antiangiogenic and antilymphangiogenic activities, thus affording it the potential to inhibit tumor lymphangiogenesis and LN metastasis. We propose that VASH1 should be tested further for controlling tumor angiogenesis and lymphangiogenesis.

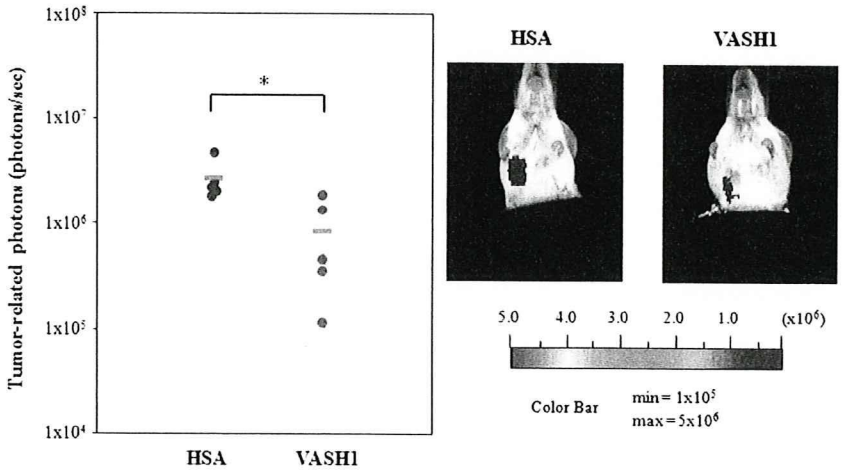

Figure 8. VASH1 inhibits LN metastasis of orthotopically inoculated 231LN-Luc-1 cells. 231LN-Luc-1 cells (5×10^6) were inoculated into the abdominal mammary fat pad of mice. Recombinant VASH1 protein or HSA was applied locally. Auxiliary LN metastasis was analyzed by the bioluminescence imaging technique. LN metastasis on day 32 was quantified as photons/sec on the left. $n = 5$, $^*P < 0.05$. Representative photos on day 32 are shown on the right. The color-bar indicates the value (photons/sec) for metastatic tumors.

Acknowledgments

We thank Yuriko Fujinoya and Kyoko Shimizu for their excellent technical assistance.

References

1. Oliver G, Alitalo K: The lymphatic vasculature: recent progress and paradigms. Annu Rev Cell Dev Biol 2005, 21:457–483
2. Alitalo K, Tammela T, Petrova TV: Lymphangiogenesis in development and human disease. Nature 2005, 438:946–953
3. Leong SP, Cady B, Jablons DM, Garcia-Aguilar J, Reintgen D, Jakub J, Pendas S, Duhaime L, Cassell R, Gardner M, Giuliano R, Archie V, Calvin D, Mensha L, Shivers S, Cox C, Werner JA, Kitagawa Y, Kitajima M: Clinical patterns of metastasis. Cancer Metastasis Rev 2006, 25:221–232
4. Adams RH, Alitalo K: Molecular regulation of angiogenesis and lymphangiogenesis. Nat Rev Mol Cell Biol 2007, 8:464–478
5. Cao R, Eriksson A, Kubo H, Alitalo K, Cao Y, Thyberg J: Comparative evaluation of FGF-2-, VEGF-A-, and VEGF-C-induced angiogenesis, lymphangiogenesis, vascular fenestrations, and permeability. Circ Res 2004, 94:664–670
6. Cao R, Bjorndahl MA, Religa P, Clasper S, Garvin S, Galter D, Meister B, Ikomi F, Tritsaris K, Dissing S, Ohhashi T, Jackson DG, Cao Y: PDGF-BB induces intratumoral lymphangiogenesis and promotes lymphatic metastasis. Cancer Cell 2004, 6:333–345
7. Bjorndahl M, Cao R, Nissen LJ, Clasper S, Johnson LA, Xue Y, Zhou Z, Jackson D, Hansen AJ, Cao Y: Insulin-like growth factors 1 and 2 induce lymphangiogenesis in vivo. Proc Natl Acad Sci USA 2005, 102:15593–15598
8. Cao R, Bjorndahl MA, Gallego MI, Chen S, Religa P, Hansen AJ, Cao Y: Hepatocyte growth factor is a lymphangiogenic factor with an indirect mechanism of action. Blood 2006, 107:3531–3536
9. Sato Y: Update on endogenous inhibitors of angiogenesis. Endothelium 2006, 13:147–155
10. Hawighorst T, Oura H, Streit M, Janes L, Nguyen L, Brown LF, Oliver G, Jackson DG, Detmar M: Thrombospondin-1 selectively inhibits early-stage carcinogenesis and angiogenesis but not tumor lymphangiogenesis and lymphatic metastasis in transgenic mice. Oncogene 2002, 21:7945–7956
11. Fukumoto S, Morifuji M, Katakura Y, Ohishi M, Nakamura S: Endostatin inhibits lymph node metastasis by a down-regulation of the vascular endothelial growth factor C expression in tumor cells. Clin Exp Metastasis 2005, 22:31–38
12. Brideau G, Makinen MJ, Elamaa H, Tu H, Nilsson G, Alitalo K, Pihlajaniemi T, Heljasvaara R: Endostatin overexpression inhibits lymphangiogenesis and lymph node metastasis in mice. Cancer Res 2007, 67:11528–11535
13. Watanabe K, Hasegawa Y, Yamashita H, Shimizu K, Ding Y, Abe M, Ohta H, Imagawa K, Hojo K, Maki H, Sonoda H, Sato Y: Vasohibin as an endothelium-derived negative feedback regulator of angiogenesis. J Clin Invest 2004, 114:898–907
14. Shibuya T, Watanabe K, Yamashita H, Shimizu K, Miyashita H, Abe M, Moriya T, Ohta H, Sonoda H, Shimosegawa T, Tabayashi K, Sato Y: Isolation and characterization of vasohibin-2 as a homologue of VEGF-inducible endothelium-derived angiogenesis inhibitor vasohibin. Arterioscler Thromb Vasc Biol 2006, 26:1051–1057
15. Kimura H, Miyashita H, Suzuki Y, Kobayashi M, Watanabe K, Sonoda H, Ohta H, Fujiwara T, Shimosegawa T, Sato Y: Distinctive localization and opposed roles of vasohibin-1 and vasohibin-2 in the regulation of angiogenesis. Blood 2009, 113:4810–4818
16. Shen JK, Yang XR, Sato Y, Campochiaro PA: Vasohibin is up-regulated by VEGF in the retina and suppresses VEGF receptor 2 and retinal neovascularization. FASEB J 2006, 20:723–725
17. Yamashita H, Abe M, Watanabe K, Shimizu K, Moriya T, Sato A, Satomi S, Ohta H, Sonoda H, Sato Y: Vasohibin prevents arterial neointimal formation through angiogenesis inhibition. Biochem Biophys Res Commun 2006, 345:919–925
18. Hosaka T, Kimura H, Heishi T, Suzuki Y, Miyashita H, Ohta H, Sonoda H, Moriya T, Suzuki S, Kondo T, Sato Y: Vasohibin-1 expressed in endothelium of tumor vessels regulates angiogenesis. Am J Pathol 2009, 175:430–439
19. Sonoda H, Ohta H, Watanabe K, Yamashita H, Kimura H, Sato Y: Multiple processing forms and their biological activities of a novel angiogenesis inhibitor vasohibin. Biochem Biophys Res Commun 2006, 342:640–646
20. Kern J, Steurer M, Gasti G, Gunsilius E, Untergasser G: Vasohibin inhibits angiogenic sprouting in vitro and supports vascular maturation processes in vivo. BMC Cancer 2009, 9:284
21. Bjorndahl MA, Cao R, Burton JB, Brakenhielm E, Religa P, Galter D, Wu L, Cao Y: Vascular endothelial growth factor-A promotes peritumoral lymphangiogenesis and lymphatic metastasis. Cancer Res 2005, 65:9261–9268
22. Chang LK, Garcia Cardena G, Farnebo F, Fannon M, Chen EJ, Butterfield C, Moses MA, Mulligan RC, Folkman J, Kaipainen A: Dose-dependent response of FGF-2 for lymphangiogenesis. Proc Natl Acad Sci USA 2004, 101:11658–11663
23. Kozaki K, Miyaishi O, Tsukamoto T, Tatematsu Y, Hida T, Takahashi T, Takahashi T: Establishment and characterization of a human lung cancer cell line NCI-H460-LNM35 with consistent lymphogenous metastasis via both subcutaneous and orthotopic propagation. Cancer Res 2000, 60:2535–2540
24. Schledzewski K, Falkowski M, Moldenhauer G, Metharom P, Kzhyshkowska J, Ganss R, Demory A, Falkowska-Hansen B, Kurzen H, Ugurel S, Geginat G, Arnold B, Goerdt S: Lymphatic endothelium-specific hyaluronan receptor LYVE-1 is expressed by stabilin-1+, F4/80+, CD11b+ macrophages in malignant tumours and wound healing tissue in vivo and in bone marrow cultures in vitro: implications for the assessment of lymphangiogenesis. J Pathol 2006, 209:67–77
25. Hirakawa S, Brown LF, Kodama S, Paavonen K, Alitalo K, Detmar M: VEGF-C-induced lymphangiogenesis in sentinel lymph nodes promotes tumor metastasis to distant sites. Blood 2007, 109:1010–1017
26. Harrell MI, Iritani BM, Ruddell A: Tumor-induced sentinel lymph node lymphangiogenesis and increased lymph flow precede melanoma metastasis. Am J Pathol 2007, 170:774–786
27. Hong YK, Shin JW, Detmar M: Development of the lymphatic vascular system: a mystery unravels. Dev Dyn 2004, 231:462–473
28. Hirakawa S, Kodama S, Kunstfeld R, Kajiya K, Brown LF, Detmar M: VEGF-A induces tumor and sentinel lymph node lymphangiogenesis and promotes lymphatic metastasis. J Exp Med 2005, 201:1089–1099
29. Schoppmann SF, Birner P, Stockl J, Kalt R, Ullrich R, Caucig C, Kriehuber E, Nagy K, Alitalo K, Kerjaschki D: Tumor-associated macrophages express lymphatic endothelial growth factors and are related to peritumoral lymphangiogenesis. Am J Pathol 2002, 161:947–956
30. Cursiefen C, Chen L, Borges LP, Jackson D, Cao J, Radziejewski C, D'Amore PA, Dana MR, Wiegand SJ, Streilein JW: VEGF-A stimulates lymphangiogenesis and hemangiogenesis in inflammatory neovascularization via macrophage recruitment. J Clin Invest 2004, 113:1040–1050
31. Murakami M, Zheng Y, Hirashima M, Suda T, Morita Y, Ooehara J, Ema H, Fong GH, Shibuya M: VEGFR1 tyrosine kinase signaling promotes lymphangiogenesis as well as angiogenesis indirectly via macrophage recruitment. Arterioscler Thromb Vasc Biol 2008, 28:658–664
32. Padera TP, Kadambi A, di Tomaso E, Carreira CM, Brown EB, Boucher Y, Choi NC, Mathisen D, Wain J, Mark EJ, Munn LL, Jain RK: Lymphatic metastasis in the absence of functional intratumor lymphatics. Science 2002, 296:1883–1886
33. Casanovas O, Hicklin DJ, Bergers G, Hanahan D: Drug resistance by evasion of antiangiogenic targeting of VEGF signaling in late-stage pancreatic islet tumors. Cancer Cell 2005, 8:299–309
34. Bergers G, Hanahan D: Modes of resistance to anti-angiogenic therapy. Nat Rev Cancer 2008, 8:592–603
35. Hwang RF, Yokoi K, Bucana CD, Tsan R, Killion JJ, Evans DB, Fidler IJ: Inhibition of platelet-derived growth factor receptor phosphorylation by STI571 (Gleevec) reduces growth and metastasis of human pancreatic carcinoma in an orthotopic nude mouse model. Clin Cancer Res 2003, 9:6534–6544
36. Nissen LJ, Cao R, Hedlund EM, Wang Z, Zhao X, Wetterskog D, Funa K, Brakenhielm E, Cao Y: Angiogenic factors FGF2 and PDGF-BB synergistically promote murine tumor neovascularization and metastasis. J Clin Invest 2007, 117:2766–2777
37. He Y, Kozaki K, Karpanen T, Koshikawa K, Yla-Herttuala S, Takahashi T, Alitalo K: Suppression of tumor lymphangiogenesis and lymph node metastasis by blocking vascular endothelial growth factor receptor 3 signaling. J Natl Cancer Inst 2002, 94:819–825

Cancer Science
The official journal of the Japanese Cancer Association JCA

Vasohibin-1 as a potential predictor of aggressive behavior of ductal carcinoma *in situ* of the breast

Kentaro Tamaki,[1,7] Hironobu Sasano,[2] Yohei Maruo,[2] Yayoi Takahashi,[2] Minoru Miyashita,[1,2] Takuya Moriya,[3] Yasufumi Sato,[4] Hisashi Hirakawa,[5] Nobumitsu Tamaki,[6] Mika Watanabe,[2] Takanori Ishida[1] and Noriaki Ohuchi[1]

[1]Department of Surgical Oncology, Tohoku University Graduated School of Medicine, Miyagi; [2]Department of Pathology, Tohoku University Hospital, Miyagi; [3]Department of Pathology 2, Kawasaki Medical School, Okayama; [4]Department of Vascular Biology, Institute of Development, Aging and Cancer, Tohoku University, Miyagi; [5]Department of Surgery, Tohoku Kosai Hospital, Miyagi; [6]Department of Breast Surgery, Nahanishi Clinic, Okinawa, Japan

(Received October 19, 2009/Revised December 14, 2009/Accepted December 17, 2009/Online publication February 5, 2010)

Vasohibin-1 is a recently identified negative feedback regulator of angiogenesis induced by VEGF-A and bFGF. In this study, we first evaluated mRNA expression of vasohibin-1 and CD31 in 39 Japanese female breast carcinoma specimens including 22 invasive ductal carcinoma (IDC) and 17 ductal carcinoma *in situ* (DCIS) using a real-time quantitative RT-PCR (QRT-PCR) with LightCycler system. In addition, we also immunolocalized vasohibin-1 and CD31 and compared their immunoreactivity to nuclear grades and histological grades of 100 carcinoma cases (50 IDC and 50 DCIS). There were no statistically significant differences of CD31 mRNA expression and the number of CD31 positive vessels between DCIS and IDC ($P = 0.250$ and $P = 0.191$, respectively), whereas there was a statistically significant difference in vasohibin-1 mRNA expression and the number of vasohibin-1 positive vessels in DCIS and IDC ($P = 0.022$ and $P \leq 0.001$, respectively). There was a significant positive correlation between vasohibin-1 mRNA level and Ki-67 labeling index in DCIS ($r^2 = 0.293$, $P \leq 0.001$). In addition, vasohibin-1 mRNA expression was correlated with high nuclear and histological grades in DCIS cases and a significant positive correlation was detected between the number of vasohibin-1 positive vessels and Ki-67 labeling index or nuclear grade or Van Nuys classification of carcinoma cells ($P \leq 0.001$, respectively). These results all indicate the possible correlation between aggressive biological features in DCIS including increased tumor cell proliferation and the status of neovascularization determined by vasohibin-1 immunoreactivity. (*Cancer Sci* 2010; 101: 1051–1058)

Breast cancer is one of the most common malignancies in woman worldwide and its morbidity has recently increased.[1] Numerous factors have been reported to be associated with development of breast cancer including angiogenesis. Angiogenesis or the formation of new blood vessel networks not only plays a pivotal role in human normal development, but also in pathological conditions such as inflammatory diseases and neoplasms.[2] A switch to the actively angiogenic phenotype is in general considered to be dependent upon an *in situ* balance between stimulatory and inhibitory factors of angiogenesis.[2,3] Therefore, numerous studies have been reported on the mechanisms of control or regulation of angiogenesis since the discovery of endothelium-specific proangiogenic factors, namely vascular endothelial growth factor (VEGF) and angiopoietin family proteins.[2] In addition, other molecules involved in this process of angiogenesis, including pigment epithelium derived factor (PEDF), platelet factor 4, angiostantin and endostatin, have been proposed as angiogenesis inhibitors.[2,4]

Vasohibin-1 has been very recently identified as one of the first established negative feedback regulators of angiogenesis, from an extensive microarray analysis originally designed to identify genes up-regulated by VEGF in cultured vascular endothelial cells.[2,5–8] Vasohibin-1 was subsequently demonstrated to be specifically expressed in ECs and its expression increased in response to angiogenic stimulators such as VEGF and basic fibroblastic growth factor (bFGF).[5,8] Vasohibin-1 is also abundantly present in human placenta and fetus,[4,5,7] in which angiogenic events markedly occur *in vivo*, but controversies exist as to whether this is the cases in all these tissues. Vasohibin-1 inhibits growth, migration, and network formation of endothelial cells and works in an autocrine manner as negative feedback regulators for angiogenesis.[8] Signals mediated by VEGF-A, one of the known VEGF family members, are transduced via VEGF receptor 2 (Flk-1),[9] and protein kinase C δ (PKCδ), one of the factors located in important downstream of intrasignaling pathway of Flk-1. These intracellular signals also markedly induced vasohibin-1 expression[6] but the status of vasohibin-1 in human malignancies has not necessarily been examined in detail with an exception of a few studies.[10,11]

We previously reported immunolocalization of vasohibin-1 in human breast disorders including carcinoma in order to examine whether this factor is expressed in endothelial cells or not in human breast tissues.[11] Vasohibin-1 immunodensity obtained by employing histomorphometry was significantly higher in invasive ductal carcinoma (IDC) than in ductal carcinoma *in situ* (DCIS)[11] and results of double immunostaining analysis further demonstrated that the Ki-67 labeling index among vasohibin-1 positive endothelial cells was significantly higher than that in all CD31 positive endothelial cells.[11] These results all indicated that vasohibin-1 is considered a more appropriate biomarker for intratumoral neovascularization compared to frequently employed CD31, and also demonstrated that the anti-angiogenic compensatory mechanisms may also work in invasive breast carcinoma, possibly in response to an induction of angiogenesis by various factors associated with the process of carcinoma invasion into the surrounding stromal tissue.[11] In addition, an evaluation of the number of vasohibin-1 positive vessels in human breast carcinoma turned out one of the prognostic markers for metastasis and prognosis of the patients with IDC.[11]

mRNA expression of this important regulator of angiogenesis, vasohibin-1, has, however, not been evaluated in any of the human malignancies. In addition, the status of vasohibin-1 has not been well-characterized in non-invasive human tumors. DCIS is by definition not associated with stromal invasion but its biological potentials of invasion have been always in dispute.[12,13] DCIS is also classified into several types based on its potential to recur or develop into invasive carcinoma.[12] The correlation between these phenotypes and the status of neovascularization of each cases, however, has been little examined in DCIS. Therefore, in this study, we first evaluated mRNA expression of both CD31 and vasohibin-1 in both invasive and non-invasive breast carcinomas using the LightCycler system

[7]To whom correspondence should be addressed.
E-mail: nahanisikenta@yahoo.co.jp

doi: 10.1111/j.1349-7006.2009.01483.x

technology[14,15] and then studied the correlation between the status of neovascularization and histological phenotypes of DCIS.

Materials and Methods

Breast tissue specimens. We retrieved 100 Japanese female cases of breast tissue (50 IDC and 50 DCIS) which had been operated in 2007 and 2008 at Department of Breast and Endocrine Surgery, Tohoku University Hospital and Department of Surgery, Tohoku Kosai Hospital, both located in Sendai, Japan. We received informed consents from the patients and the protocol for this study was approved by the Ethics Committee at Tohoku University Graduated School of Medicine and Tohoku Kosai Hospital (2008-472). After surgical resection of the primary tumors and gross inspection by a pathologist, all the cases had been fixed in 10% buffered formalin and embedded in paraffin, or a representative portion of the tumors of 39 cases (22 IDC and 17 DCIS) were immediately snap-frozen and stored in liquid nitrogen and stored at −80°C until use. Of the remaining 100 patients, 50 were diagnosed histopathologically as IDC and 50 as DCIS.

Real-time QRT-PCR for vasohibin-1. Thirty-nine cases of frozen sections were stained with H&E for confirmation of the presence of carcinoma cells in the specimens examined. Total RNA was extracted from primary tumors using the TRIzol reagent (Invitrogen Corpolation, Carlsbag, CA, USA), and the Transcriptor First standard cDNA Synthesis Kit (Roche Diagnostics GmbH, Mannheim, Germany) was used in the synthesis of cDNA. Real-time quantitative RT-PCR was performed on the LightCycler System (Roche Diagnostics GmbH) and the Fast Start DNA Master SYBR Green1 (Roche Diagnostics GmbH). Characteristics of the primer sequences used in this study were summarized in Table 1.[5,6,16,17] Settings for the PCR thermal profile were as follows: initial denaturation at 95°C for 10 min, followed by 40 amplification cycles of 95°C for 10 s, annealing at 62°C (vasohibin-1), 62°C (CD31) and 62°C (ribosomal protein L 13a [RPL13A]) for 10 s, respectively, and elongation at 72°C for 12 s. The cDNA of known concentrations for target genes and the housekeeping gene, RPL13A, were used to generate standard curves for quantitative PCR in order to determine the quantity of target cDNA transcripts. Quantitative normalization of each target genes in each tissue sample was performed using the expression of RPL13A mRNA as an internal control and evaluated as a ratio compared with the average expression ratio of CD31 and vasohibin-1 in DCIS cases (the averages of CD31/RPL13A and vasohibin-1/RPL13A in DCIS cases), respectively.[18–20] PCR was set up at 2 mM MgCl2, (Vasohibin,CD31), 3 mM (RPL13A) and 10 pmol/μL of each primer. The information of primers used in this study is summarized in Table 2.

Immunohistochemistry. We performed immunohistochemical staining for vasohibin-1, CD31 and Ki-67 for all cases. The specimens had been fixed in 10% formalin, embedded in paraffin, cut into 4 μm thick sections and placed on the glue-coated glass slides. Sections were deparafinized in xylene, and hydrated with graded alcohols and distilled water. Endogenous peroxidase activity was blocked by 3% hydrogen peroxidase for 10 min at room temperature. Antigen retrieval was performed using Autoclave in 10 mmol EDTA (pH 8) for vasohibin-1 and in citrate buffer for CD31 and Ki-67, heated at 121°C for 5 min. Sections were subsequently incubated for 30 min at room temperature (RT) in a blocking solution of 10% rabbit serum (Nichirei Biosciences, Tokyo, Japan), and then immunostained for over night at 4°C with primary antibodies. The primary antibodies of vasohibin-1, CD31 and Ki-67 were mouse monoclonal antibodies, and were used as follows: anti-human vasohibin-1 monoclonal antibody[9] diluted at 1:3200, anti-CD31 (Dako, Copenhagen, Denmark) diluted at 1:400 and Ki-67 (Dako) diluted at 1:300. Anti-human vasohibin-1 monoclonal antibody (mAb) was raised against the synthetic fragment (Gly286-Arg299) of human vasohibin-1 as described by Watanabe *et al.*[5] The specificity and sensitivity of this mAb was confirmed by both Western blotting and immunohistochemical analysis.[5] For vasohibin-1, CD31 and Ki-67 immunohistochemistry, secondary antibody reactions were performed using biotinyted rabbit anti-mouse antibody (Nichirei Bioscience) was used according to the manufacture's instructions. Reacted sections were visualized using 3,3′-Diaminobezidine (DAB)/30% H_2O_2 in 0.05 mol/L Tris buffer (pH 7.6) and couterstained with hematoxylin for nuclear stain.

Immunohistochemical analysis. Two of the authors independently evaluated immunoreactivity. They were blinded to the

Table 1. Clinicopathological features of the cases examined

	A	B
Histologic type		
IDC	50	22
DCIS	50	17
Nuclear grade		
IDC		
Grade 1	5	2
Grade 2	22	12
Grade 3	23	8
DCIS		
Grade 1	16	1
Grade 2	27	12
Grade 3	7	4
Histological grade		
Nottingham histological grade		
Grade 1	18	6
Grade 2	27	10
Grade 3	5	6
Van Nuys classification		
Group 1	24	8
Group 2	18	5
Group 3	8	4

A, 10% formalin fixed and paraffin embedded specimens. B, frozen sections.

Table 2. Primer sequences used in real-time PCR in this study

Gene (accession no.)	Primer for PCR	Size (bp)	Reference
CD31 (NM000442)	Forward: GATGTCAGAAACCATGCAA Reverse: AGCCTTCCGTTCTAGAGTATC	199	
Vasohibin-1 (KIAA1036)	Forward: AGATCCCCATACCGAGTGTG Reverse: GGGCCTCTTTGGTCATTTCC	167	Watanabe *et al.*[4]
RPL13A (NM012423)	Forward: CCTGGAGGAGAAGAGGAAAAG Reverse: TTGAGGACCTCTGTGTATTT	125	Vandesompele *et al.*[43]

doi: 10.1111/j.1349-7006.2009.01483.x

clinical course of the patients and the average of numbers counted by two investigators was used for subsequent analysis. Olympus BX 50 (Olympus, Tokyo, Japan) and 20× objective were used for the analysis. The number of microvessels was counted within the tumor of IDC, whereas in DCIS, the number of vessels in the stroma among intradutal components was evaluated. Microvessels were identified based on the architecture, lumen lined by endothelial cells, complemented by positivity of the endothelial cells with anti-CD31 after scanning the immunostaining section at low magnification (×40 and ×100).[21,22] The areas with greatest number of distinctly highlighted microvessels were selected, and counted at one high power (×200).[21,22] Any immunostained endothelial cells or clusters separated from adjacent vessels were counted as a single microvessels, even in the absence of vessel lumen. Each single count is defined as the highest number of microvessels identified at the "hot spot". Vasohibin-1 positive signals were counted in "hot spot" in which the highest number of anti-CD31 positive vessels was identified.[11] An evaluation of Ki-67 immunoreactivity was performed at high power field (×400) and used as a marker of cell proliferation. More than 500 tumor cells from each of three different representative fields were evaluated and the labeling index was subsequently obtained.

Statistical analysis. Statistical analysis, such as the One-factor ANOVA and Simple regression analysis, were performed using StatMate III for Windows v3.18 (ATMS Co. Ltd. Tokyo, Japan). The results were considered significant when the *P*-value were <0.05.

Results

CD31 and vasohibin-1 mRNA in breast cancers. We first examined mRNA expression of CD31 and vasohibin-1 in both IDC and DCIS. The mRNA expression of CD31 evaluated by Light Cycler ranged from 0.03 to 2.57 (median: 0.68, average: 0.86) in all the cases examined, from 0.03 to 2.32 (median: 0.84, average: 1.00) in DCIS cases, and from 0.04 to 2.57 (median: 0.61, average: 0.74) in IDC cases. There were no statistically significant differences of CD31 mRNA between DCIS and IDC cases ($P = 0.250$) (Fig. 1A). The mRNA expression of vasohibin-1 evaluated by Light Cycler ranged from 0.003 to 4.29 (median: 1.00, average: 1.44) in all the cases examined, from 0.003 to 3.28 (median: 0.68, average: 1.00) in DCIS cases, and from 0.44 to 4.28 (median: 1.71, average: 1.78) in IDC cases. There was a statistically significant difference of vasohibin-1 expression between IDC and DCIS ($P = 0.022$) (Fig. 1B).

CD31 and vasohibin-1 immunohistochemistry. The representative findings for HE, CD31 and vasohibin-1 are illustrated in Figure 2. The average number of microvessels detected by CD31 was 22.9 ± 8.5 in all cases, 21.8 ± 8.8 in DCIS and 24.0 ± 8.0 in IDC, respectively. No statistically significant differences were detected between DCIS and IDC in CD31 immunoreactivity ($P = 0.191$). Vasohibin-1 positive microvessels in "hot spot" were 15.97 ± 8.9 in all cases, 12.4 ± 9.0 in DCIS and 19.5 ± 7.3 in IDC, respectively. There was a statistically significant difference of the number of vasohibin-1 positive microvessels between DCIS and IDC ($P \leq 0.001$).

Concordance between mRNA expression and immunoreactivity of CD31 and vasohibin-1. A statistically significant positive correlation was detected between mRNA expression and immunohistochemical status in CD31 and vasohibin-1 in our present study ($P < 0.001$, respectively).

Correlation between CD31 or vasohibin-1 mRNA and Ki-67 labeling in carcinoma cells. No significant correlations were detected between the mRNA expression level of CD31 and Ki-67 labeling index of carcinoma cells in all the cases ($r^2 = 0.015$, $P = 0.453$) (Fig. 3A), in DCIS ($r^2 = 0.110$, $P = 0.194$) (Fig. 3B) and in IDC ($r^2 = 0.048$, $P = 0.329$) (Fig. 3C), respectively. However, a statistically significant positive correlation was detected between the mRNA expression level of vasohibin-1 and Ki-67 labeling index of carcinoma cells in all cases ($r^2 = 0.293$, $P < 0.001$) (Fig. 3D) and in DCIS ($r^2 = 0.466$, $P = 0.002$) (Fig. 3E). In addition, a positive correlation was also detected in IDC but the correlation did not reach statistical significance ($r^2 = 0.149$, $P = 0.08$) (Fig. 3F).

Correlation between CD31 or vasohibin-1 positive vessels and Ki-67 labeling in carcinoma cell. No significant correlations were detected between the CD31 positive vessels and Ki-67 labeling index of carcinoma cells in all the cases ($r^2 = 0.022$, $P = 0.144$) (Fig. 4A), in DCIS ($r^2 = 0.062$, $P = 0.079$) (Fig. 4B) and in IDC ($r^2 = 0.001$, $P = 0.801$) (Fig. 4C), respectively. However, a statistically significant positive correlation was detected between the vasohibin-1 positive vessels and Ki-67 labeling index of carcinoma cells in all cases ($r^2 = 0.300$, $P \leq 0.001$) (Fig. 4D),

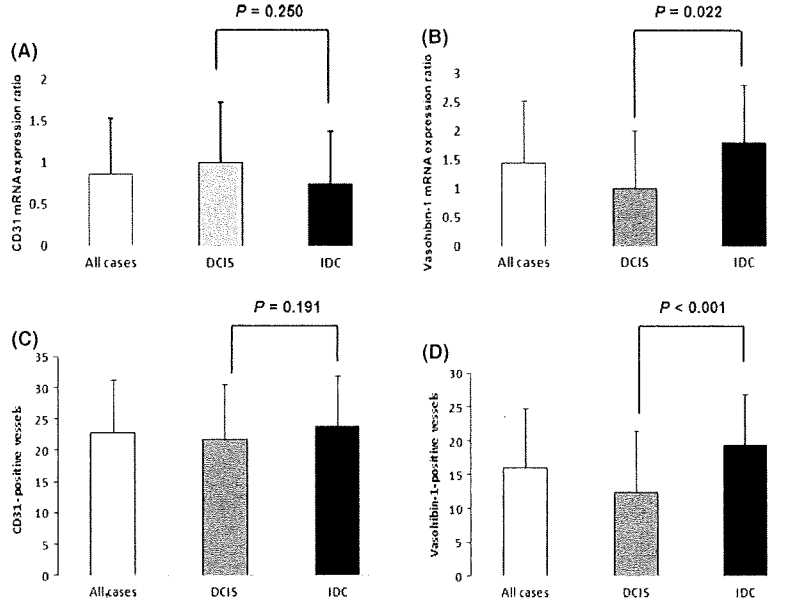

Fig. 1. The summary of analysis of mRNA expression of CD31 and vasohibin-1 in breast cancers and the number of CD31 and vasohibin-1 positive vessels. (A) represents CD31 mRNA expression ratio or level in all the cases, DCIS and IDC. (B) represents vasohibin-1 mRNA expression ratio or level in all the cases examined, DCIS and IDC. (C) represents CD31 positive vessels in all cases, DCIS and IDC. (D) represents vasohibin-1 positive vessels in all cases, DCIS and IDC.

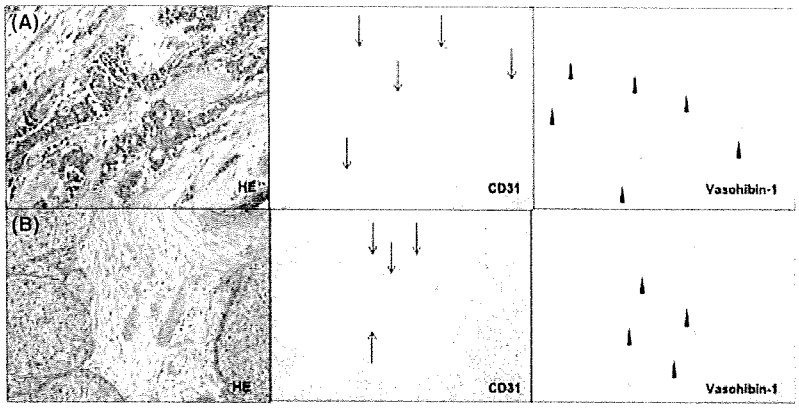

Fig. 2. Representative illustrations of histological and immunohistochemical findings of breast carcinoma cases examined. Original magnification is x200. (A) corresponded to DCIS and (B) to IDC. These cases were stained positively for both CD31 (↓) and vasohibin-1 (↑).

in DCIS ($r^2 = 0.521$, $P \leq 0.001$) (Fig. 4E) and in IDC ($r^2 = 0.278$, $P \leq 0.001$) (Fig. 4F), respectively.

Correlation between vasohibin-1 mRNA expression and nuclear grade of carcinoma cells. The mRNA expression level of vasohibin-1 ranged from 0.47 to 0.81 (median: 0.55, average: 0.61) in NG (nuclear grade) 1 carcinoma cases, from 0.003 to 4.29 (median: 0.94, average: 1.14) in NG2 carcinoma cases and from 0.44 to 3.54 (median: 2.15, average: 2.24) in NG3 cases. There were statistically significant differences of vasohibin-1 mRNA levels between NG1 and NG3 ($P = 0.003$), and NG2 and NG3 ($P = 0.01$), whereas no significant differences were detected between NG1 and NG2 ($P = 0.374$) in all cases (Fig. 5A).In DCIS, a significant difference was detected between NG2 (ranged from 0.003 to 1.27, median: 0.55, average: 0.54) and NG3 (ranged from 1.34 to 3.28, median: 2.15, average: 2.50) in DCIS ($P < 0.001$) (Fig. 5B), whereas there were no statistically significant differences between NG2 (ranged from 0.49 to 4.29, median: 1.15, average: 1.75) and NG3 (ranged from 0.44 to 3.54, median: 2.03, average: 2.11) in IDC ($P = 0.444$) (Fig. 5C).

Correlation between the number of vasohibin-1 positive vessels and nuclear grade of carcinoma cells. The number of vasohibin-1 positive vessels was 8.0 ± 9.6 in NG1, 16.4 ± 6.9 in NG2 and 20.9 ± 7.5 in NG3 in all DCIS cases examined, respectively (Fig. 5D). There were significant differences among the different nuclear grades of all the cases examined ($P \leq 0.001$ between NG1 and the other grades, $P = 0.003$ between NG2 and NG3, respectively). The number of vasohibin-1 positive vessels was significantly different among DCIS cases with different nuclear grades (3.7 ± 2.7 in NG1, 13.8 ± 6.1 in NG2 and 27.3 ± 4.3 in NG3 in DCIS cases, respectively, $P \leq 0.001$) (Fig. 5E). In addition, the number of vasohibin positive vessels in IDC cases with different nuclear grades was 18.0 ± 7.0 in NG1, 27.1 ± 7.7 in NG2 and 21.6 ± 6.2 in NG3 in IDC cases, respectively (Fig. 5F). Statistically significant differences were not detected among these cases of IDC ($P = 0.559$ between NG1 and NG2, $P = 0.746$ between NG2 and NG3, $P = 0.469$ between NG1 and NG3).

Correlation between vasohibin-1 mRNA and Van Nuys classification for DCIS, and Nottingham histological grade for IDC. In DCIS cases, the mRNA expression levels of vasohibin-1 ranged from 0.06 to 1.13 (median: 0.48, average: 0.52) in Group 1, from 0.003 to 1.27 (median: 0.55, average: 0.57) in Group 2 and from 1.34 to 3.28 (median: 2.15, average: 2.50) in Group 3 of Van Nuys Classification. There were statistically significant differences between Group 1 and Group 3 ($P < 0.001$), and Group 2 and Group 3 ($P = 0.005$), respectively. No statistically significant differences were detected between Group 1 and Group 2 ($P = 0.832$) (Fig. 6A). In IDC cases, the mRNA expression level of vasohibin-1 ranged from 0.55 to 2.52 (median: 1.00, average: 1.32) in HG (histological grade) 1, from 0.44 to 4.29 (median: 1.11, average: 1.58) in HG2 and from 1.58 to 3.54 (median: 2.40, average: 2.44) in HG3. A statistical significance was identified only between HG1 and HG3 cases of IDC ($P = 0.03$). No significant differences were detected between HG1 and HG2 ($P = 0.692$), and HG2 and HG3 ($P = 0.154$) IDC cases, respectively (Fig. 6B).

Correlation between vasohibin-1 positive vessels and Van Nuys classification for DCIS, and Nottingham hisotological grade for IDC. In DCIS cases, the number of vasohibin-1 positive vessels was 7.5 ± 5.6 in Group 1, 13.1 ± 7.8 in Group 2 and

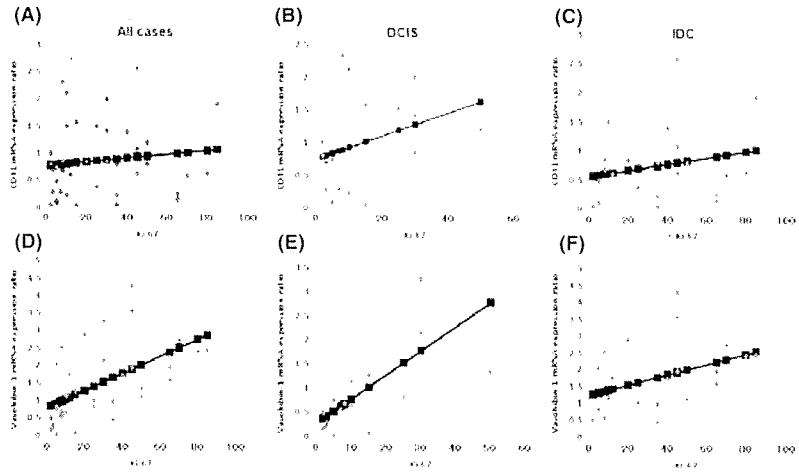

Fig. 3. (A), (B) and (C) represent the results of the correlation between Ki-67 labeling index and CD31 mRNA expression ratio or level. (A) represents all the cases, (B) DCIS and (C) IDC. (D), (E) and (F) represent the results of the correlation between Ki-67 labeling index and vasohibin-1 mRNA expression level or ratio. (D) all cases, (E) DCIS and (F) IDC.

doi: 10.1111/j.1349-7006.2009.01483.x

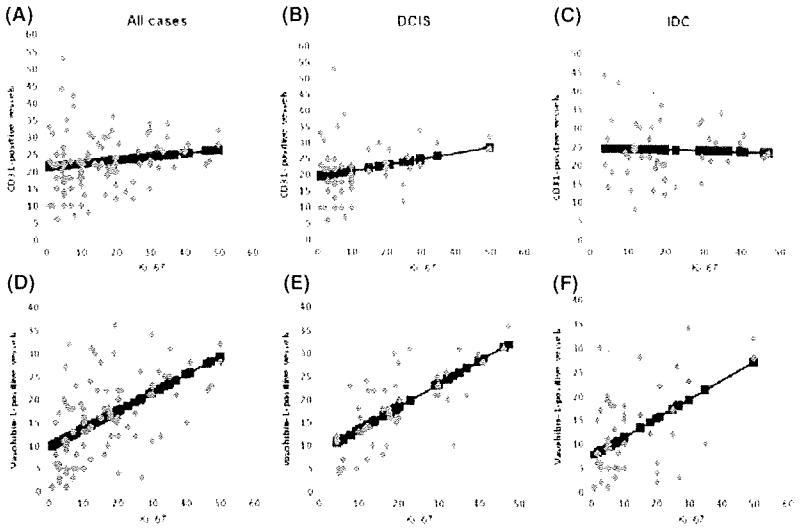

Fig. 4. (A), (B) and (C) represent the results of the correlation between Ki-67 labeling index and CD31 positive vessels. (A) represents all the cases, (B) DCIS and (C) IDC. (D), (E) and (F) represent the correlation between Ki-67 labeling index and vasohibin-1 positive vessels. (D) all cases, (E) DCIS and (F) IDC.

26.0 ± 5.0 in Group 3 of Van Nuys classification, respectively (Fig. 6C). Statistically significant differences were also detected among the different groups according to Van Nuys classification, respectively ($P \leq 0.001$ between Group 3 and the other groups, $P = 0.009$ between Group 1 and Group 2). In IDC cases, the number of vasohibin-1 positive vessels was 18.0 ± 7.0 in HG1, 20.1 ± 7.7 in HG2 and 21.6 ± 6.2 in HG3. No significant differences were detected among the different grades of IDC cases, respectively ($P = 0.357$ between HG1 and HG2, $P = 0.688$ between HG2 and HG3, $P = 0.310$ between HG1 and HG3) (Fig. 6D).

Discussion

Angiogenesis, the formation of new blood vessels from the existing vascular network, represents a complex multi-step process involving extracellular matrix remodeling, endothelial cell migration and proliferation, capillary differentiation and anastomosis. Angiogenesis is a pivotal event in various biological processes in both physiological and pathological settings. Physiological conditions include embryonic development, reproduction, and wound healing; whereas pathologic conditions include cancers, proliferative retinopathy, and rheumatoid arthritis. *In situ* balance between angiogenesis stimulators such as VEGF and bFGF and inhibitors such as thrombospondin-1 (TSP-1) and pigment epithelium derived factor (PEDF) is generally considered to regulate the process of angiogenesis.[3] Previous studies demonstrated that vasohibin-1 expression is induced in endothelial cells after stimulation with VEGF-A or bFGF and that these factors also stimulate proliferation and migration of endothelial cells.[2,4–6] The endothelium-derived negative feedback regulators of angiogenesis have not been elucidated until the discovery or identification of vaohibin-1. Therefore, vasohibin-1 is the first secretory anti-angiogenic factor from endothelial cells themselves.[2,4–6]

Results of our previous study[11] was the first to examine the status of vasohbin-1 in human breast diseases in which angiogenesis also plays important roles. In particular, results of double immunostaining analysis demonstrated the significant positive correlation between Ki-67 positive proliferating vascular endothelial cells, which may represent neovascular formation[23,24] and vasohibin-1 positive endothelial cells.[10] The Ki-67 labeling index among vasohibin-1 positive endothelial cells was significantly higher than that in all CD31 positive endothelial cells.[11] These results all indicated that vasohibin-1 is considered a more appropriate biomarker for neovascularization compared to

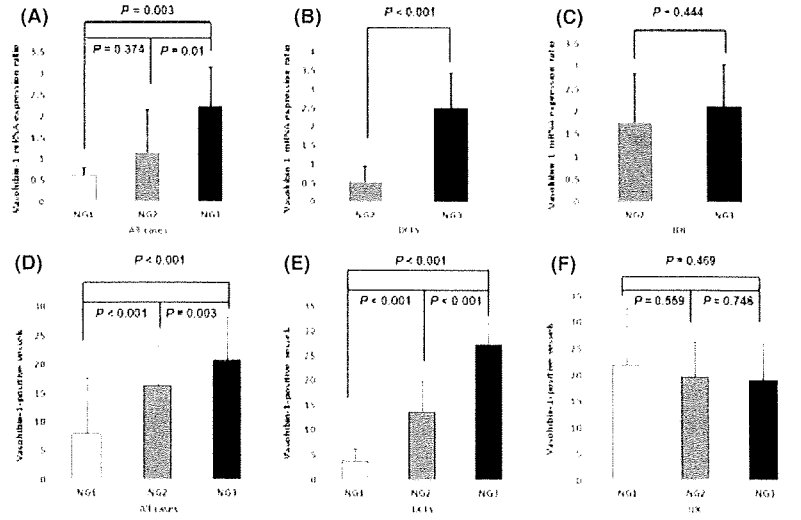

Fig. 5. (A), (B) and (C) represent summary of results of the correlation between vasohibin-1 mRNA expression level or ratio and nuclear grade. (A) all the cases, (B) DCIS and (C) IDC. (D), (E) and (F) represent summary of results of the correlation between vasohibin-1 positive vessels and nuclear grade. (D) all cases, (E) DCIS and (F) IDC.

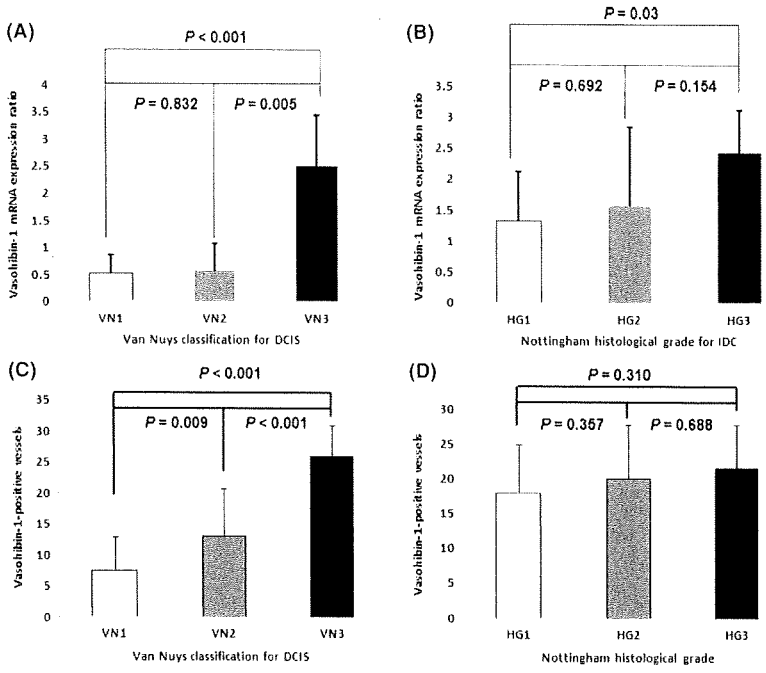

Fig. 6. (A) and (B) represent the analysis of correlation between vasohibin-1 mRNA expression ratio and histological grade. (A) with Van Nuys classification for DCIS and (B) with Nottingham histological grades for IDC. (C) and (D) represent the analysis of correlation between vasohibin-1 positive vessels and histological grade. (C) with Van Nuys classification for DCIS cases and (D) with Nottingham histological grades for IDC cases.

CD31, which may detect all the vasculature including both resting and proliferating endothelial cells.[11] However it is known that vasohibin-1 is inhibitor for neovascularization, the high vasohibin-1 expression is related with high neovascularization and worse prognostic factors. It is all suggest that the effect of angiogenesis is higher than the anti-angiogenic effect of vasohibin-1 in high grade malignant cases.

To the best of our knowledge, this is the first reported study evaluating vasohibin-1 gene expression in human malignancies. Results of our present study demonstrated that mRNA expression of vasohibin-1 tended to be higher in IDC than DCIS, but no differences of CD31 mRNA were detected between these invasive and non-invasive lesions. These findings also indicated that the anti-angiogenic compensatory mechanism through *in situ* production of vasohibin-1 may play important roles in invasive breast carcinoma, possibly in response to an induction of angiogenesis by various factors related to carcinoma invasion into the surrounding stroma.

DCIS constitutes a spectrum of non-invasive proliferative epithelial lesions with a predilection for the terminal duct-lobular units of the breast.[25] DCIS is in general considered a precursor of IDC and is defined as a lesion in which carcinoma cells do not usually grow beyond the basal membrane of the mammary duct.[26] Many factors including nuclear grade, adhesion, tumor cell proliferation, and neovascularizasion have been proposed to be associated with the process of carcinoma cell invasion in breast stroma or development from DCIS to IDC.[12,27–29] For instance, Kerilkowske *et al.* demonstrated that nuclear grade is the best indicator of recurrence and progression to invasive carcinoma in DCIS cases.[12] Lightfoot *et al.* also demonstrated that the expression of focal adhesion kinase (FAK) was associated with tumor cell invasion in the progression of DCIS.[27] In addition, Shen *et al.* reported that tumor cells in DCIS are required not only to increase their proliferative capacity but also to escape program cell death control for development to invasive carcinoma.[28] The proliferation of small subsets of tumor cells is initially limited by the distance from basement membrane when invasion occurs in DCIS.[30] The presence of an increased vascular density suggestive of neovascularization around DCIS has been reported in a number of reported studies.[29,31,32] In addition, the possible association between higher vascularity and increased incidence of stromal invasion or recurrence has been also proposed in the cases with DCIS.[29] Results of these reported studies all indicated that a putative angiogenic switch or alteration in DCIS may contribute to the transformation from *in situ* to invasive carcinoma. In addition, results of previous studies demonstrated that different expression patterns of angiogenesis factors in low-grade as opposed to high-grade DCIS is consistent with the concept that characteristic pathways exist in an evolution from DCIS to invasive breast cancer.[33,34]

This is the first study to examine the vasohibin-1 expression in DCIS, in detail. Our previous study demonstrated that the cases with a higher number of vasohibin-1 positive vessels tended to be associated with better and statistically significant OS and DFS in invasive breast cancer. In addition, we also reported that vasohibin-1 immunodensity was significantly higher in IDC than in DCIS. We therefore considered vasohibin-1 as a more appropriate biomarker for intratumoral neovascularization than CD31. These results also suggested that vasohibin-1 may be induced in the spectrum of of the stromal or host reaction to carcinoma cells infiltration into stroma. Angiogenesis in invasive breast cancer has been well documented but relatively fewer studies have examined the possible roles of angiogenesis in pre-invasive ductal diseases or in what stages the angiogenic switches may occur during the process of breast carcinoma development.[35] Results of several previous studies demonstrated that the significant increment in the percentage of MVD was detected in high grade *in situ* breast carcinoma.[30,35–36] In addition, higher histological and nuclear grades in DCIS cases were also reported to be significantly associated with higher microvessel counts, and subsequently higher potential of invasive transformation.[37]

Results of our present study did demonstrate high vasohibin-1 expression in a number of DCIS cases. A significant positive correlation was detected between the vasohibin-1 expression and Ki-67 labeling index of carcinoma cells in DCIS. In addition, a relatively higher level of vasohibin-1 expression was detected in DCIS cases associated with high nuclear and histological grades than those with low nuclear and histological grades. Pure DCIS without any foci of stromal invasion does not

doi: 10.1111/j.1349-7006.2009.01483.x

generally have the potential to metastasize.[30] Therefore, the particular clinical importance of DCIS is the risk of developing into invasive carcinoma.[30] Results of our present study demonstrated that increased vasohibin-1 expression was associated with both increased cell proliferation of carcinoma cells and higher nuclear and histological grades. Therefore, these results clearly indicated that vasohibin-1 expression level in DCIS could become one of the appropriate biomarker of the potential of subsequent stromal invasion of carcinoma cells but further studies including those examining DCIS cases with known clinical outcome are required for clarification.

It has been clearly demonstrated that cancer development requires neovascularization.[30] Angiogenic pathway is also well-known to become more numerous and redundant as breast cancer progresses as in other human malignancies.[38] Therefore, an inhibition of a single factor or pathway may not necessarily result in sustained clinical therapeutic efficacy in the patients with previously treated, highly refractory diseases. Recently, newer targeted therapies toward the control of tumor neovascularization such as anti-VEGF therapy have been developed in phase II and III clinical trials of breast cancer patients.[39–42] These agents generally demonstrated the clinical effects such as reduction of neoplastic angiogenesis and inhibition of solid tumors proliferation, either alone or in combination with chemotherapy.[39–42] The most important factor in the development of these therapies is obviously a detailed investigation of angiogenic mechanism, with an emphasis on studying biological features of newly formed vessels. Results of our present study as well as of previous studies[2–8,10,11] studied angiogenic mechanism through vasohibin-1 and vasohibin-1 itself could be considered a candidate of anti-VEGF and anti-angiogenesis agent to administer adequately to control tumor angiogenesis.

Acknowledgments

We appreciate Katsuhiko Ono, MT, for his excellent technical assistance. This work was partly supported by the grants from the Japanese Ministry of Health, Labour and Welfare for Researches on Intractable Diseases, Risk Analysis Research on Food and Pharmaceuticals, and Development of Multidisciplinary Treatment Algorithm with Biomarkers and Modeling of the Decision-making Process with Artificial Intelligence for Primary Breast Cancer. This work was also partly supported by Grant-in-Aid for Scientific Research (18390109) from the Japanese Ministry of Education, Culture, Sports, Science and Technology, and the Yasuda Medical Foundation.

References

1 Kamangar F, Dores GM, Anderson WF. Patterns of cancer incidence, mortality, and prevalence across five continents: defining priorities to reduce cancer disparities in different geographic regions of the world. *J Clin Oncol* 2006; **24**: 2137–50.
2 Sato Y, Sonoda H. The vasohibin family: a negative regulatory system of angiogenesis generally programmed in endothelial cells. *Arterioscl Thromb Vasc Biol* 2007; **27**: 37–41.
3 Folkman J. Angiogenesis in cancers, vascular, rheumatoid and other disease. *Nat Med* 1995; **1**: 27–31.
4 Sato Y. Update on endogenous inhibitors of angiogenesis. *Endothelium* 2006; **13**: 147–55.
5 Watanabe K, Hasegawa Y, Yamashita H *et al.* Vasohibin as an endothelium-derived negative feedback regulator of angiogenesis. *J Clin Invest* 2004; **114**: 898–907.
6 Shimizu K, Watanabe K, Yamashita H *et al.* Gene regulation of novel angiogenesis inhibitor, vasohibin, in endothelial cells. *Biochem Biophys Res Commun* 2005; **327**: 700–6.
7 Kerbel RS. Vasohibin: the feedback on a new inhibitor of angiogenesis. *J Clin Invest* 2004; **114**: 884–6.
8 Sonoda H, Ohta H, Watanabe K *et al.* Multiple processing forms and their biological activities of a novel angiogenesis inhibitor vasohibin. *Biochem Biophys Res Commun* 2006; **342**: 640–6.
9 Ferrara N. Vascular endothelial grpwth factor: basic science and clinical progress. *Endocr Rev* 2004; **25**: 581–611.
10 Yoshinaga K, Ito K, Moriya T *et al.* Expression of vasohibin as a novel endothelium-derived angiogenesis inhibitor in endometrial cancer. *Cancer Sci* 2008; **99**: 914–9.
11 Tamaki K, Moriya T, Sato Y *et al.* Vasohibin-1 in human breast carcinoma: a potential negative feedback regulator of angiogenesis. *Cancer Sci* 2009; **100**: 88–94.
12 Kerlikowske K, Molinaro A, Cha I *et al.* Characteristics associated with recurrence among women with ductal carcinoma in situ treated by lumpectomy. *J Natl Cancer Inst* 2003; **95**: 1692–702.
13 Chapman JA, Miller NA, Lickley HL *et al.* Ductal carcinoma in situ of the breast (DCIS) with heterogeneity of nuclear grade: prognostic effects of quantitative nuclear assessment. *BMC Cancer* 2007; **7**: 174.
14 Wittwer CT, Ririe KM, Andrew RV *et al.* The LightCycler: a microvolume multisample fluorimeter with rapid temperature control. *Biotechniques* 1997; **22**: 176–81.
15 Bernard PS, Wittwer CT. Real-time PCR technology for cancer diagnostics. *Clin Chem* 2002; **48**: 1178–85.
16 Hida K, Hida Y, Amin DN *et al.* Tumor-associated endothelial cells with cytogenetic abnormalities. *Cancer Res* 2004; **64**: 8249–55.
17 Suzuki T, Miki Y, Moriya T *et al.* Estrogen-relate receptor alpha in human breast carcinoma as a potent prognostic factor. *Cancer Res* 2004; **64**: 4670–6.
18 Ohtani S, Kagawa S, Tango Y *et al.* Quantitative analysis of p53-targeted gene expression and visualization of p53 transcriptional activity following intratumoral administration of adenoviral p53 in vivo. *Mol Cancer Ther* 2004; **3**: 93–100.
19 Williams NS, Gaynor RB, Scoggin S *et al.* Identification and validation of genes involved in the pathogenesis of colorectal cancer using cDNA microarrays and RNA interference. *Clin Cancer Res* 2003; **9**: 931–46.
20 Nakamura Y, Suzuki S, Suzuki T *et al.* MDM2: a novel mineralocoticoid-responsive gene involved in aldosterone-induced human vascular structural remodeling. *Am J Pathol* 2006; **169**: 362–71.
21 Weidner N, Semple JP, Welch WR *et al.* Tumor angiogenesis and metastasis-correlation in invasive breast carcinoma. *N Engl J Med* 1991; **324**: 1–8.
22 Weidner N, Folkman J, Pozza F *et al.* Tumor angiogenesis: a new significant and independent prognostic indicator in early-stage breast carcinoma. *J Natl Cancer Inst* 1992; **84**: 1875–87.
23 Nijsten T, Copaert CG, Vermeulen PB *et al.* Cyclooxygenase-2 expression and angiogenesis in squamous cell carcinoma of the skin and its precursors: a paired immunohistochemical study of 36 cases. *Br J Dermatol* 2004; **151**: 837–45.
24 Hoskin PJ, Sibtain A, Daley FM *et al.* The immunohistochemical assessment of hypoxia, vascularity and proliferation in bladder carcinoma. *Radiother Oncol* 2004; **72**: 159–68.
25 The Consensus Conference Committee (Contact: Dr Gordon F. Schwartz). Consensus conference on the classification of ductal carcinoma in situ. *Cancer* 1997; **80**: 1798–802.
26 Page DL, Dupont WD, Rogers LW *et al.* Intraductal carcinoma of the breast: follow-up after biopsy only. *Cancer* 1982; **49**: 751–8.
27 Lightfoot HM Jr, Lark A, Livasy CA *et al.* Upregulation of focal adhesion kinase (FAK) expression in ductal carcinoma in situ (DCIS) is an early event in breast tumorigenesis. *Breast Cancer Res Treat* 2004; **88**: 109–16.
28 Shen KL, Harn HJ, Ho LI *et al.* The extent of proliferative and apoptotic activity in intraductal and invasive ductal breast carcinomas detected by Ki-67 labeling and terminal deoxynucleotidyl transferase-mediated digoxigenin-11-dUTP nick end labeling. *Cancer* 1998; **82**: 2373–81.
29 Teo NB, Shoker BS, Jarvis C *et al.* Angiogenesis and invasive recurrence in ductal carcinoma in situ of the breast. *Eur J Cancer* 2003; **39**: 38–44.
30 Wulfing P, Kersting C, Buerger H *et al.* Expression patterns of angiogenic and lymphangiogenic factors in ductal breast carcinoma in situ. *Br J Cancer* 2005; **92**: 1720–8.
31 Engels K, Fox SB, Whitehouse RM *et al.* Distinct angiogenic patterns are associated with high-grade in situ ductal carcinoma of the breast. *J Pathol* 1997; **181**: 207–12.
32 Guidi AJ, Schnitt SJ, Fischer L *et al.* Microvessel density distribution in ductal carcinoma in situ of the breast. *J Natl Cancer Inst* 1994; **86**: 614–9.
33 Buerger H, Otterbach F, Simon R *et al.* Different genetic pathway in the evolution of invasive breast cancer are associated with distinct morphological subtypes. *J Pathol* 1999; **189**: 521–6.
34 Mommers EC, Leonhart AM, Falix F *et al.* Similarity in expression of cell cycle proteins between in situ and invasive ductal breast lesions of same differentiation grade. *J Pathol* 2001; **194**: 327–33.

35 Bluff JE, Menakuru SR, Cross SS *et al.* Angiogenesis is associated with the onset of hyperplasia in human ductal breast disease. *Br J Cancer* 2009; **101**: 666–72.
36 Pavlakis K, Messini I, Vrekoussis T *et al.* The assessment of angiogenesis and fibroblastic stromagenesis in hyperplastic and pre-invasive lesions. *BMC Cancer* 2008; **8**: 88.
37 Cao Y, Paner GP, Kahn LB, Rajan PB. Noninvasive carcinoma of the breast. Angiogenesis and cell proliferation. *Arch Pathol Lab Med* 2004; **128**: 893–6.
38 Relf M, LeJeune S, Scott PA *et al.* Expression of the angiogenic factors vascular endothelial cell growth factor, acidic and basic fibroblast growth factor, tumor growth factor beta-1, platelet-derived endothelial cell growth factor, placenta growth factor, and pleiotrophin in human primary breast cancer and its relation to angiogenesis. *Cancer Res* 1997; **57**: 963–9.
39 Rugo HS. Bevacizumab in the treatment of breast cancer: rationale and current data. *The Oncologist* 2004; **9**: 43–9.
40 Fox SB, Generali DG, Harris AL. Breast tumour angiogenesis. *Breast Cancer Res* 2007; **9**: 216.
41 Miller KD, Chap LI, Holmes FA *et al.* Randomized phase III trial of capecitabine compared with bevacizumab plus capecitabine in patients with previously treated metastatic breast cancer. *J Clin Oncol* 2005; **23**: 792–9.
42 Wedam SB, Low JA, Yang SX *et al.* Antiangiogenic and antitumor effects of bevacizumab in patients with inflammatory and locally advanced breast cancer. *J Clin Oncol* 2006; **24**: 769–77.

doi: 10.1111/j.1349-7006.2009.01483.x

Cancer Science
The official journal of the Japanese Cancer Association JCA

Pigpen, a nuclear coiled body component protein, is involved in angiogenesis

Tomoko Yoshida,[1] Yasufumi Sato,[3] Ikuo Morita[2] and Mayumi Abe[1,4]

Departments of [1]Nanomedicine (DNP) and [2]Cellular Physiological Chemistry, Graduate School of Medical and Dental Sciences, Tokyo Medical and Dental University, Tokyo; [3]Department of Vascular Biology, Institute of Development, Aging and Cancer, Tohoku University, Sendai, Japan

(Received November 2, 2009/Revised January 3, 2010/Accepted January 6, 2010)

We previously reported that puromycin-insensitive leucyl-specific aminopeptidase (PILSAP) is required for vascular endothelial growth factor (VEGF)- and basic fibroblast growth factor (bFGF)-induced angiogenesis and for endothelial differentiation from embryonic stem (ES) cells via the aminopeptidase activity of PILSAP. In this study, we searched for molecules that function during angiogenesis with PILSAP. We performed proteome analysis of nuclear extracts from embryoid bodies (EBs) made from ES cells transfected with mutant PILSAP lacking aminopeptidase activity and mock EBs. We identified pigpen, a 67-kDa nuclear coiled body component protein. Immunoprecipitation and western blotting demonstrated the binding of PILSAP and pigpen in endothelial cells (ECs), and this interaction was enhanced by VEGF and bFGF. Pigpen was reported to be expressed in actively growing ECs such as those in embryos and tumors. However, whether Pigpen is involved in angiogenesis is not known. Therefore, we examined the effect of pigpen on angiogenesis by silencing pigpen with siRNA (siPigpen). Compared with scrambled RNA (scrPigpen), transfection of siPigpen into mouse ECs inhibited proliferation, migration, and network formation. These results were confirmed with other two siRNAs. Moreover, siPigpen suppressed bFGF-induced angiogenesis in a Matrigel plug assay, and injection of siPigpen into Lewis lung carcinoma cell tumors implanted subcutaneously into 5-week-old C57/BL male mice prevented tumor growth and tumor angiogenesis. These data indicate that Pigpen is involved in angiogenesis and that pigpen may be a target for blocking tumor angiogenesis. (*Cancer Sci* 2010)

New blood vessel formation or angiogenesis is clinically classified into two types, physiological and pathological angiogenesis. Pathological angiogenesis is indispensable for tumor growth and metastasis.[1] To induce angiogenesis, tumors secrete various growth factors and proteolytic enzymes that stimulate endothelial cells (ECs), mobilize endothelial progenitor cells (EPCs) from bone marrow, and degrade the extracellular matrix (ECM) including the basement membrane.[2] Therefore, anti-angiogenic drugs have been developed to inhibit tumor angiogenesis by targeting ECs. Some angiogenesis inhibitors have been approved for use in progressive or metastatic tumors in combination with chemotherapy. Angiogenesis can be inhibited by blocking angiogenesis factors or their receptors, blocking signaling pathways, or by mimetics or derivatives of endogenous angiogenesis inhibitors. Currently, the most promising target is vascular endothelial growth factor (VEGF). The importance of VEGF has been further demonstrated by the observation that VEGF haploinsufficiency in mice is embryonically lethal due to a defect in blood vessel formation.[3,4]

Using PCR-coupled subtractive cDNA cloning, we previously isolated genes that are expressed during *in vitro* differentiation of mouse embryonic stem (ES) cells to ECs and identified puromycin-insensitive leucyl-specific aminopeptidase (PILSAP), whose expression is induced by VEGF.[5] We further demonstrated that PILSAP plays an important role in postnatal angiogenesis.[5] VEGF facilitates PILSAP binding to its substrate, phosphatidylinositol-dependent kinase 1 (PDK1) via aminopeptidase (AP) activity, allowing complex formation of PILSAP-PDK1-S6 kinase (S6K) and resulting in activation of cyclin-dependent kinase (CDK) 4/6 by phosphorylated S6K. Activated CDK 4/6 then promotes G1–S transition, leading to EC proliferation.[6] PILSAP is also involved in VEGF-mediated induction of EC migration by activating integrins and focal adhesion kinase[7] as well as increasing adhesion of ECs to the ECM via activation of RhoA.[8]

In this study, we searched for molecules that interact with PILSAP and function in angiogenesis, and identified pigpen using proteome analysis of mtPILSAP-EBs lacking AP activity[9] and mock EBs. Pigpen is a 67-kDa sepharose-binding molecule that was previously isolated from ECs[10] and is a nuclear coiled body component protein.[11,12] The Cajal bodies, or coiled bodies (CBs) were first discovered as nuclear accessory bodies by Ramóny Cajal and were found to be ubiquitous nuclear inclusions of unknown function.[12] CBs are enriched in rapidly dividing cells with high levels of transcriptional activities.[13] Since the component proteins of CBs such as coilin and the survival of motor neurons (SMN) have been identified, the research into CBs has been greatly advanced and suggests that CBs are involved in coordinating the assembly and maturation of nuclear ribonucleoproteins (RNPs). On the other hand, little is known about the function of another CB component protein, pigpen. However, pigpen is demonstrated to be expressed also in actively growing cells such as ECs in embryos and tumors.[10,14] Nuclear injection of anti-pigpen antibodies inhibits EC division,[15] and therefore pigpen may play a role in angiogenesis. To clarify whether and how pigpen is involved in angiogenesis, we synthesized siRNAs for pigpen. Transfection of the siRNA inhibited angiogenesis *in vivo* as well as *in vitro*. Furthermore, siPigpen inhibited tumor angiogenesis and tumor growth in a mouse syngeneic tumor transplant model. These results indicate that pigpen plays a role in angiogenesis via induction of EC proliferation, migration, and network formation, and may be a future target for blocking tumor angiogenesis.

Materials and Methods

Cell culture. Mock and mtPILSAP ES cells were produced and cultured as previously described.[9] The mouse endothelial cell lines MSS31 and MS1 were cultured in alpha MEM (αMEM; Invitrogen Life Technologies, Carlsbad, CA, USA) with 10% FBS and high glucose DMEM (HG-DMEM; Invitrogen) with 5% FBS, respectively. Lewis lung carcinoma cells (LLC) were cultured in DMEM (Invitrogen) with 10% FBS.

ES *in vitro* differentiation culture system. *In vitro* differentiation of mock and mtPILSAP ES cells in methylcellulose was performed as previously described.[9] Cells were harvested from

[4]To whom correspondence should be addressed.
E-mail: mayumidnp@tmd.ac.jp

doi: 10.1111/j.1349-7006.2010.01494.x

the culture on day 8 for proteome analysis and immunoprecipitation followed by western blotting (IP-Western).

Proteome analysis. Nuclear protein from day 8 mock and mtPILSAP EBs was purified, and the protein concentration was measured using a Bio-Rad Dc Protein Assay Kit (Bio-Rad Laboratories, Hercules, CA, USA). Proteome analysis using 20 μg each of nuclear protein was conducted by AMR (Tokyo, Japan).

IP-Western. Polyclonal rabbit IgG against a synthetic peptide corresponding to amino acid residues 262–275 of mouse pigpen, including a cysteine linker (RDQGSRHDSEQDNSC), was prepared (anti-mPigpen Ab). MSS31 cells were starved in αMEM with 0.1% BSA (BSA-αMEM) for 24 h and incubated in BSA-αMEM with 50 ng/mL VEGF (Sigma, St. Louis, MO, USA) or 20 ng/mL basic fibroblast growth factor (bFGF; BD Biosciences, San Jose, CA, USA) for 20 min. The cell extract (500 μg) was incubated with 10 μg antimouse PILSAP goat IgG (anti-mPILSAP Ab; R&D Systems, Minneapolis, MN, USA) for 13 h at 4°C. Immune complexes were incubated with protein G-sepharose (GE Healthcare Life Science, Uppsala, Sweden) for 2 h at 4°C. Immunoprecipitates were applied to a western blot with 2 μg/mL anti-mPILSAP Ab or anti-mPigpen Ab. The signals were detected with ECL plus western blotting detection reagents (GE Healthcare) and visualized using LAS1000 (Fuji, Tokyo, Japan).

Immunocytochemistry (ICC). MSS31 cells were starved in αMEM containing 0.1% FBS (0.1% αMEM) for 24 h and incubated in 0.1% αMEM with 50 ng/mL VEGF or 20 ng/mL bFGF for 20 min. Cells were fixed in 4% paraformaldehyde (PFA), incubated in blocking solution (BS: 2% BSA and 0.2% Triton X-100 in PBS) at room temperature (RT:18–24°C) for 30 min, and treated with 10 μg/mL anti-mouse PILSAP goat IgG or normal goat IgG (Santa Cruz Biotechnology, Santa Cruz, CA, USA) in 1/10 (v/v) BS (reaction buffer; RB) at 4°C overnight, followed by incubation with 4 μg/mL Alexa568-conjugated donkey antigoat IgG (Invitrogen) in RB at RT for 1 h. Cells were then incubated firstly with 10 μg/mL antimouse pigpen rabbit IgG or normal rabbit IgG (Santa Cruz Biotechnology) in RB at RT for 1 h and then with 4 μg/mL Alexa488-

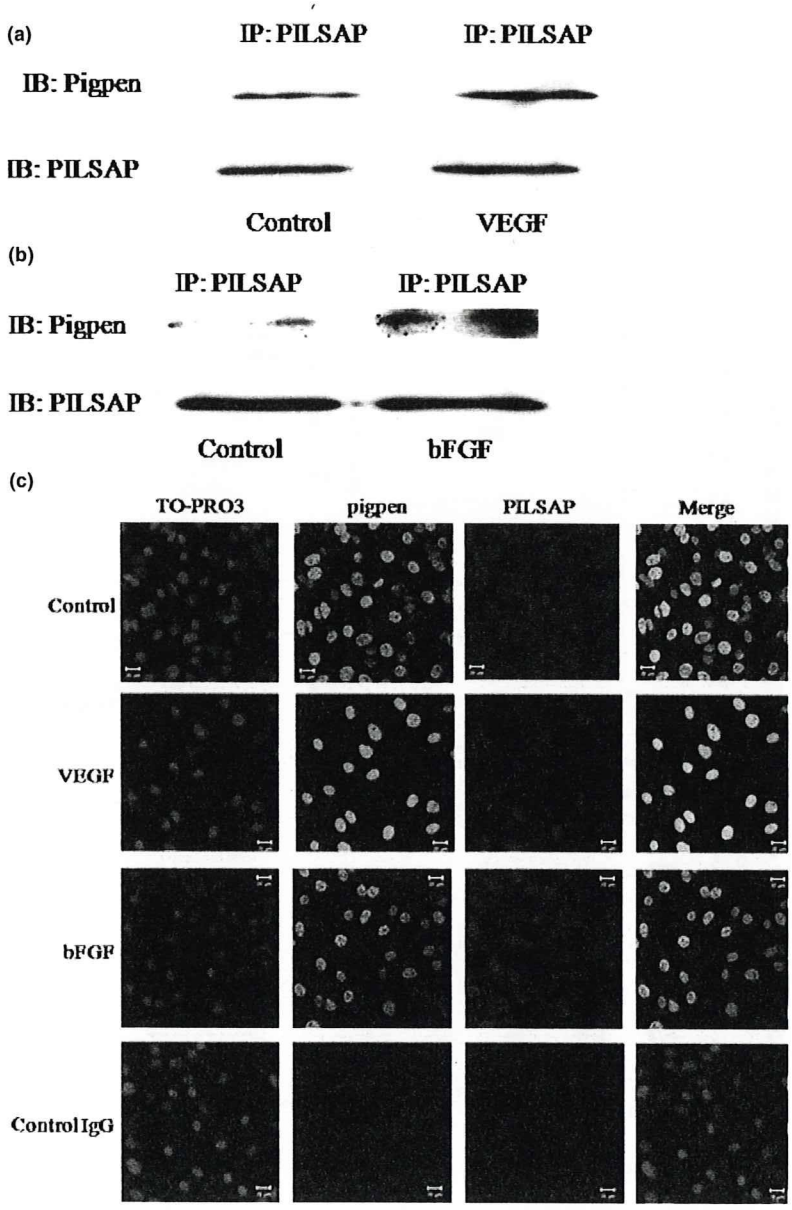

Fig. 1. Immunopreciptation by anti-puromycin-insensitive leucyl-specific aminopeptidase (PILSAP) Ab followed by western blotting of pigpen and PILSAP (a,b) and immunocytochemistry of pigpen (green) and PILSAP (red) (c) in MSS31 cells treated with vehicle, 50 ng/mL vascular endothelial growth factor (VEGF), or 20 ng/mL basic fibroblast growth factor (bFGF) for 20 min. Nuclei were counterstained with TO-PRO-3 (blue). Bars = 20 μm.

doi: 10.1 111/j.1349-7006.2010.01494.x

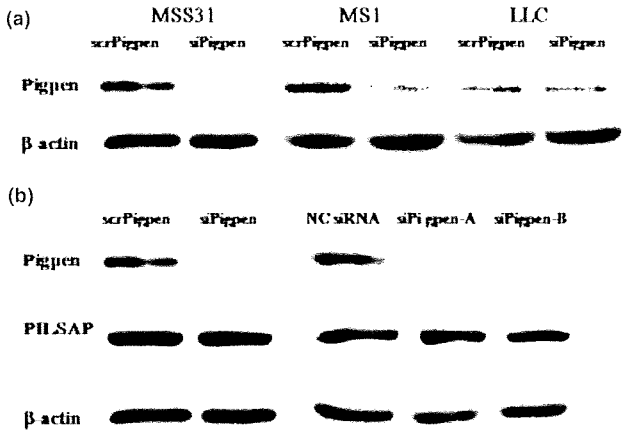

Fig. 2. Western blot of pigpen in scr- or siPigpen-transfected MSS31, MS1, and Lewis lung carcinoma (LLC) cells (a). Western blot of pigpen and PILSAP in MSS31 transfected with scr- or siPigpen, siPigpen-A, siPigpen-B, or nontargeting siRNA (NC siRNA) as a negative control for siPigpen-A and -B (b). Equal loading was confirmed by β-actin.

conjugated donkey antirabbit IgG (Invitrogen) in RB at RT for 1 h. Nuclei were stained with TO-PRO-3 (Invitrogen). Cells were washed with PBS at RT for 5 min twice between each steps. Images were photographed by a Zeiss LSM 510 confocal microscope system (Carl Zeiss, Oberkochen, Germany).

Inhibition of pigpen expression by siRNA. Control or siRNA oligonucleotides at a final concentration of 10 nM were transfected into MS1, MSS31, and LLC cells using Lipofectamine RNAiMAX Transfection Reagent (Invitrogen). The sequences of siPigpen and scrPigpen were as follows: 5′-GAACAGGAUAAUUCAGACATT-3′ and 5′-AAUCGAAUUAGCAGGAAACTT-3′, respectively. The sequences of the other set, siPigpen-A, siPigpen-B, and nontargeting control siRNA (NC siRNA) as a negative control for these two siRNAs were as follows: 5′-CAAACGACUAUACCCAACATT-3′, 5′-CAAUACCAUCUUCGUGCAATT-3′, and 5′-UCUUAAUCGCGUAUAAGGCTT-3′, respectively. The efficacy of siRNAs for pigpen was evaluated by mRNA (data not shown) and protein levels.

Western blotting. The protein extracts (20 μg) from MSS31, MS1, and LLC cells transfected with scr- or siPigpen for 24 h were applied to a western blot with 2 μg/mL anti-mPigpen Ab or anti-mPILSAP Ab. The signals were detected with ECL plus western blotting detection reagents and visualized using LAS1000. Equal loading was confirmed by blotting with anti-β-actin Ab (Sigma).

EC proliferation assay. At 24 h after transfection of scr- or siPigpen into MSS31 or LLC cells (2000 cells/well in a 96-well-plate), cells were incubated in 0.1% αMEM with or without 50 ng/mL VEGF (MSS31) or 1 or 10% DMEM for another 24 h. In some experiment, cells were transfected with scr- or siPigpen, NC siPigpen, siPigpen-A, or siPigpen-B on the day before an assay. MS1 or MSS31 cells (20 000 or 10 000/well, respectively) were inoculated in a 96-well-plate and incubated in 0.1% HG-DMEM or 0.1% αMEM. After 24-h incubation, the medium of MS1 was changed to 100 μL/well of 0.1%

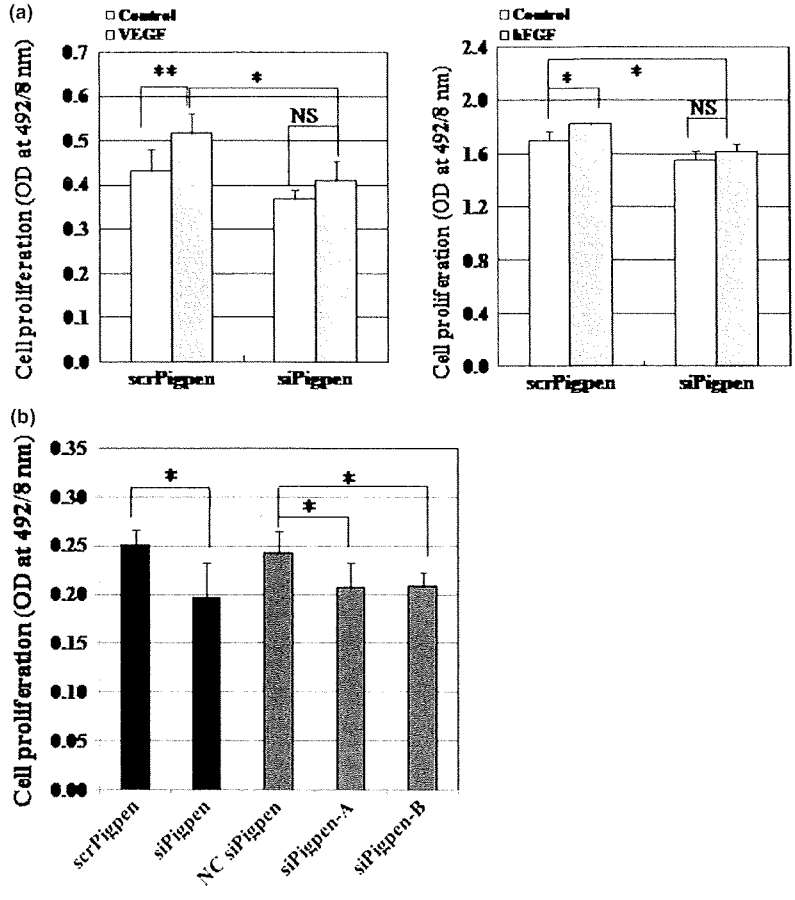

Fig. 3. (a) Endothelial cell (EC) proliferation assay of MSS31 (left) and MS1 (right) cells transfected with scr- or siPigpen. MSS31 cells were treated with or without 50 ng/mL vascular endothelial growth factor (VEGF) for 24 h ($n = 6$). MS1 cells were treated with or without 20 ng/mL basic fibroblast growth factor (bFGF) for 24 h ($n = 3$). (b) EC proliferation assay of MSS31 cells transfected with scr- or siPigpen, nontargeting control siRNA (NC siRNA), siPigpen-A, or siPigpen-B. ($n = 6$ for scr- or siPigpen and $n = 5$ for NC siRNA, siPigpen-A, or siPigpen-B). Bars indicate SDs. $^*P < 0.05$, $^{**}P < 0.01$.